Investigation of the molecular and isotopic response to deposition, thermal maturity, hydrocarbon generation, and expulsion

A multidisciplinary approach based on the Cenozoic sequences on Svalbard

Markus Dörner

Thesis for the degree of Philosophiae Doctor (PhD)
University of Bergen, Norway
2020

UNIVERSITY OF BERGEN

Investigation of the molecular and isotopic response to deposition, thermal maturity, hydrocarbon generation, and expulsion

A multidisciplinary approach based on the Cenozoic sequences on Svalbard

Markus Dörner

Thesis for the degree of Philosophiae Doctor (PhD)
at the University of Bergen

Date of defense: 20.05.2020

Year: 2020

Title: Investigation of the molecular and isotopic response to deposition, thermal maturity, hydrocarbon generation, and expulsion

Name: Markus Dörner

Print: Skipnes Kommunikasjon / University of Bergen

Preface

This thesis is submitted for the degree of Philosophiae Doctor at the University of Bergen.

The PhD project was carried out in cooperation between the Department of Chemistry of the University of Bergen and Equinor ASA, Bergen. Equinor ASA provided the funding for this project. The presented work consists of an introductory part and five research articles of which two have been published in internationally recognised peer-reviewed journals. Three additional manuscripts have been submitted to internationally recognised journals of which one was resubmitted after revision. In this thesis, chapter 1 provides a brief introduction to the research topic. Chapter 2 summarised the main research aims and questions. Chapter 3 provides the reader with a detailed overview over the analytical techniques that were used to generate the data included in this thesis. Chapter 4 is composed of a summary for each of the published and submitted manuscript, including the aims, the execution of the study and major findings. Chapter 5 provides a condensed summary of the thesis and an outlook to further work. The last part of this thesis consists of the published articles and submitted manuscripts.

All analytical work was performed in the research laboratory of Equinor ASA in Bergen, except for ICP-MS and XRF analyses which were conducted at the Department of Geoscience of the University of Bergen.

During the three and a half years of research, I had four contributions to international conferences, of which the last one is not part of this thesis. A report quoting our findings of the first publication was contained in the January edition of the German journal “Labor Praxis” in 2018.

The thesis covers topics ranging from organic and inorganic geochemistry to analytical chemistry.

Acknowledgements

First, I would like to thank my three supervisors from the University of Bergen and Equinor ASA, Tanja Barth (UiB), Michael Erdmann (Equinor), and Ulrich Berner (Equinor).

Tanja, thank you for making this project a smooth and enjoyable experience. I highly appreciate your experience in the field of organic chemistry and your hands-on handling of scientific manuscripts. Thanks for a lot of good suggestions and comments on my written work, and the support during the training component of the PhD program.

Michael, I would like to thank you for all the scientific input that I received from you during the thesis work, but also beside the topics of this project. I have learned a lot from you. I am grateful that you have initiated this project at Equinor, and I would like to thank you for all the interesting project insights that you made available to me.

Uli, I do not know where to start. I thank you for all the scientific and nonscientific discussions that we still have almost every day. Your experience in the field of organic and inorganic geochemistry is priceless and this work heavily benefited from all your input. I would also like to say thank you for making me (and my family) feel welcome in Norway from day one.

I would like to thank Siv Hjorth Dundas and the laboratory team from the Geoscience department of the University of Bergen, for conducting the ICP-MS and XRF analyses.

My colleagues and supervisors from the Equinor Laboratory and Test Facilities are thanked for great discussions, analytical and technical support, for always good mood at work and for making me learn Norwegian. You all (Anita Låstad Johnsen, Arne Hundhammer, Cato Kristoffersen, Claudia Kruber, Geir Torkildsen, Hans Kristian Hornnes, Hege Fonneland, Jan Inge Strand, Kristin Erstad, Lars Harald Heggen, Marian Våge, Tone Gulli Hæreid) contributed to this project and made my time in Norway since 2016 a great experience.

I am grateful to my family for all the support during the time at the University of Hamburg and now in Norway. Without this support it would not have been possible to finish this project.

Finally, I would like to thank my wife, Nadja. Your constant support and love during times when I was busy with writing, travelling or other project related work is what kept me going, especially during the last few months. It is incredible how you managed to stay so positive, handle your own job and the kids. Without you this would have never been possible.

Abstract

Understanding the generation, expulsion and migration of hydrocarbons and the associated effects on the molecular composition of generated products plays a major role in petroleum system analyses. The presented PhD study is based on a research well from the Central Tertiary Basin of Svalbard which has not been investigated in detail previously. The core material from this well is of exceptional quality.

A comprehensive depositional reconstruction of the lithologies of the research well has been established by combining inorganic and organic geochemistry. Shedding a light on the effects of sulphate reduction on the preserved organic matter quality supported a better understanding of the depositional settings and natural quality limitations on the present-day organic matter concentration.

The effects of thermal maturity on the organic matter and on selected biomarker compounds as well as on molecular maturity proxies has been investigated. The implementation of multivariate statistics has led to the creation of a novel unitless biomarker maturity trend.

Molecular fractionation effects associated with the expulsion and migration of hydrocarbons have been investigated. The findings show that polar compounds and asphaltenes were preferentially retained in the organic rich layers of the lower Frysjaodden Fm. On the other hand, the expelled hydrocarbons have migrated upwards and mainly consist of saturated compounds of low polarity. The development of an advanced maturity-based back-calculation approach made it possible to calculate the amounts of hydrocarbons that have been generated, expelled and migrated with respect to their initial organic matter quality and quantity.

In addition to the geoscientific investigations, two analytical methodologies have been developed in the course of this PhD project. The first methodology involves the multiple detector coupling to a single gas chromatograph in order to enhance the data density per injection and significantly reduce the sample preparation work for organic geochemical analyses. The second method is used to monitor the isotopic

composition of the Rock-Eval S1 and S2 parameters in an online analysis. This analytical setup was described for the first time. The results support a better understanding of isotopic fractionation effects introduced by thermal maturation and hydrocarbon generation and expulsion. The results from these analyses have also been used to confirm the impact of sulphate reduction on the reactive organic matter proportion in the Paleocene Eocene transition of the investigated well.

List of Publications

Paper I: Dörner, M., Berner, U., Erdmann, M., & Barth, T., (2018). Organic geochemical research analytics of the petroleum industry: enhanced data density and method flexibility using gas chromatograph multiple detector coupling. Geological Society, London, Special Publications, 484, SP484-6

Paper II: Dörner, M., Berner, U., Erdmann, M., & Barth, T., (2019). Geochemical characterization of the depositional environment of Paleocene and Eocene sediments of the Tertiary Central Basin of Svalbard. **Submitted** to Chemical Geology (under review).

Paper III: Dörner, M., Berner, U., Erdmann, M., & Barth, T., (2019). Carbon isotopic analysis of reactive organic matter using a new pyrolysis-cryotrapping-isotope ratio mass spectrometry method: The isotope variation of organic matter within the S1 and S2 peaks of Rock-Eval. Organic Geochemistry, 136, October 2019, 103886.

Paper IV: Dörner, M., Berner, U., Erdmann, M., & Barth, T., (2019). Organic geochemical characterization of hydrocarbon generation and migration at the Paleocene-Eocene transition on Svalbard. **Submitted** to Organic Geochemistry (under review).

Paper V: Dörner, M., Berner, U., Erdmann, M., & Barth, T., (2020). Qualitative evaluation of molecular maturity markers in thermally mature sediments, a case study from Svalbard. **Revised version submitted** to Organic Geochemistry (under review).

List of Conference Contributions

Not included in this thesis

Dörner, M., Berner, U., Erdmann, M., & Barth, T., (2016). OG analytics in the Petroleum industry - Enhanced data density and method flexibility by multiple detector GC coupling. Poster at the conference on Application of Analytical Techniques to Petroleum Systems Problems, 28 Feb-1 March 2017, Geological Society of London (United Kingdom)

Dörner, M., Berner, U., Erdmann, M., Dahlgren, T., & Barth, T., (2017). Primary migration and expulsion – Application of the Rock Eval Shale method and QEMSCAN observations on Cenozoic sediments from the Central Tertiary Basin of Svalbard. Poster at the Gussow Conference, Banff (Canada).

Dörner, M., Berner, U., Erdmann, M., & Barth, T., (2017). Paleoenvironmental Characterization of Thermally Mature Organic Matter Using a New Pyrolysis Method. Plenary Talk International Meeting on Organic Geochemistry (IMOG), 2017, Florence (Italy)

Dörner, M., Berner, U., Erdmann, M., & Barth, T., (2019). The PyroViewer – a new Rock-Eval data evaluation tool. Poster at the conference in Celebration of the life of Chris Cornford (1948-2017): Petroleum System Analysis ‘Science or Art?’, Geological Society of London, 24-25 April 2019, London (United Kingdom)

Contents

1. Introduction

1.1 Outline

The following chapter contains a brief introduction to the principles of hydrocarbon generation, expulsion and migration as well as the geological background of the study area and a description of the wellbore which has been used in the scientific publications produced in the course of the PhD thesis.

1.2 Hydrocarbon generation, expulsion and migration in the subsurface

1.2.1 Origin and transformation of organic matter

Elevated concentrations of organic matter are predominantly parts of fine-grained marine and lacustrine sediments, as well as swamps. Usually, such sediments are deposited in low transport energy settings. Due to both polymerisation and polycondensation, large molecules form during the diagenesis of the organic matter rich sediments. Those humic substances are the precursors for the so-called kerogen. Kerogen is a geopolymer consisting of a complex mixture of interconnected organic compounds. Kerogen is by definition neither soluble in organic solvents, nor in water. According to the specifications used by Killops and Killops (2005) there are five different kerogen types, each of which can be differentiated by its specific association to a depositional setting and its elemental composition.

Type I: Liptinite rich, typically of lacustrine origin (high H/C, low O/C ratio).

Type II: Intermediate between I and III, represents mixtures of marine organic matter mixed with terrestrial organic matter e. g. higher land plant material (high H/C, low O/C ratio).

Type II-S: Similar to II, with up to 14% organic sulphur by weight, typically affected by sulphate reduction during the deposition or other sources of sulphur, such as hydrothermal systems.

Type III: Predominantly organic matter from land plants, vitrinite macerals (H/C < 1.0, high O/C ratio),

Type IV: Largely composed of inertinite with minor vitrinite (no hydrocarbon generation potential), type IV includes highly oxidised and reworked organic matter.

The kerogen and its precursors are continuously changed during the burial process (Killops and Killops, 2005). The transformation process is initiated by microbial reworking of the organic matter during the diagenetic stage. Due to an enhanced supply of energy (heat), the transformation continuous into the catagenetic and metagenetic thermal degradation stage (Figure 1). The concept of energy supply over time is described by thermal maturation. In general, three stages of organic matter transformation with respect to the maturity level can be distinguished.

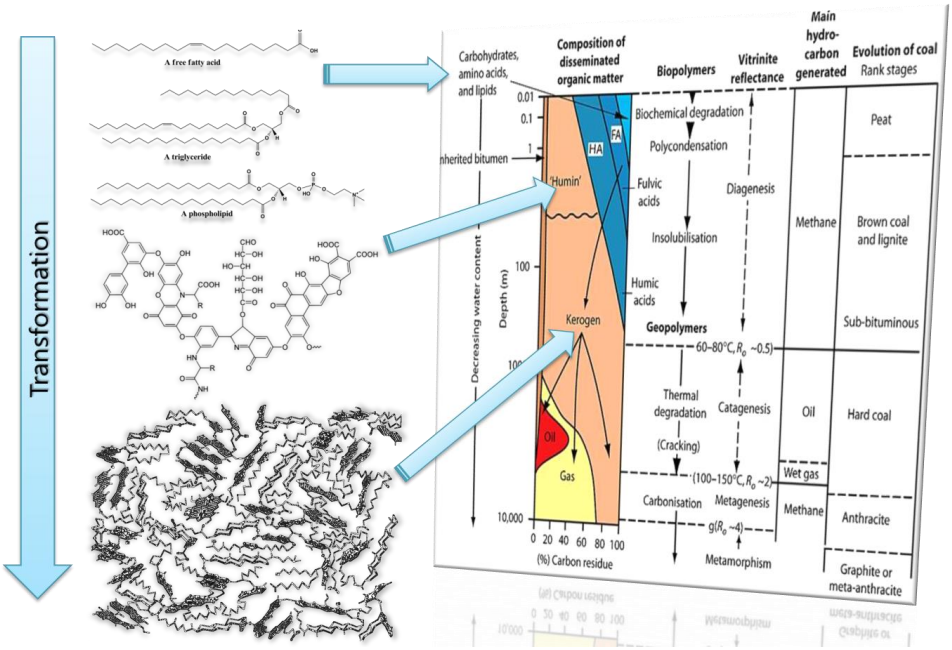

Figure 1: Transformation and maturation of organic matter as a function of depth/energy supply (picture modified after Allen and Allen, 2013*)*

Diagenesis (i): Sediments which have been deposited under subaquatic conditions usually contain a mixture of different substances. Those substances are inorganic particles (minerals), organic matter of various sources and living

microorganism. As stated by Tissot and Welte (1984), diagenesis is the process in which this highly unequilibrated mixture of different components and different origin approximates an equilibrium. The initially unconsolidated sediments become consolidated and a mild increase in temperature and pressure leads to the first transformation of the organic matter. Especially microorganisms are responsible for the initial decomposition of organic matter during the diagenesis stage. The microbial degradation process leads to the release of CO_2, NH_4, CH_4, H_2S and water.

Catagenesis (ii): As the sediments get buried deeper, a significant increase in temperature and pressure leads to the extended transformation of the organic matter which is incorporated into the sedimentary layers. The catagenetic phase marks the stage in which petroleum is generated (Horsefield and Ruellkoetter, 1994), due to the thermally induced decomposition of the kerogen. This decomposition process is mostly accomplished by the cracking of covalent C-C bonds (Vandenbroucke et al., 1993). During the catagenesis, the transformation of the organic matter leads to a constant hydrogen depletion of the residual kerogen.

Metagenesis (iii): Metagenesis marks the last stage of the thermal evolution of the organic matter. During this stage, mostly hydrocarbon gases (methane to pentane), H_2 and N_2 are released from the kerogen network through enhanced cracking (Vandenbroucke et al., 1993). When organic-rich sediments have reached the metagenetic stage, most of the liquid hydrocarbons are already expelled from the source rock, while minor amounts of generated hydrocarbons might be retained in the source rock matrix. Those retained hydrocarbons are then subjected to secondary cracking which enhances the generation of hydrocarbon gases (Killops and Killops, 2005).

1.2.2 Generation and Expulsion related fractionation

The process of primary migration or expulsion of petroleum describes the movement of generated hydrocarbons within fine-grained organic-rich rocks out of the generating strata and into adjacent lithologies (Tissot and Welte, 1984; Mann et al., 1997; Peters et al., 2005). Chemical fractionation between the bitumen phase and the

residual organic matter has been related to hydrocarbon expulsion, since petroleum reservoir fluids differ from the chemical composition of source rock extracts (Mackenzie et al., 1983, Leythaeuser et al., 1984a, b, 1988 a, b, c; Eseme et al., 2007). Significant changes in the chemical composition of hydrocarbon mixtures during the expulsion process have recently been reported for advanced laboratory experiments (Stockhausen et al., 2019) confirming the findings in natural systems and adding to a more detailed understanding of the involved processes. Chemical fractionation of the expelled organic compounds occurs when the generated fluids migrate out of the source rock and towards the adjacent rock sequences of higher porosity, permeability and lesser organic carbon contents.

In general, five different processes of expulsion and primary migration have been differentiated by Tissot and Welte (1984).

(i) Primary migration through separate petroleum droplets, (ii) primary migration through organic aggregates; (iii) primary migration of hydrocarbon compounds through the solution in pore waters, (iv) primary migration through diffusion and lastly (v) the most effective primary migration process, the so-called bulk flow or hydrocarbon phase flow.

The most relevant hydrocarbon mass transport mechanism in the subsurface is the petroleum bulk flow (England et al., 1987; Killops and Killops, 2005; Ziegs et al., 2017). This pressure-driven process requires continuous enrichment of the generated hydrocarbon in the pore space of the organic-rich source rocks. The hydrocarbons are then pushed out of the pore space into the adjacent lithologies by the elevated pressure conditions. The bulk flow can only be initiated when organic-rich source rocks produce bitumen continuously to build up a high load pressure (Tissot and Welte, 1984).

Molecular diffusion in contrast is mainly driven by concentration gradients between areas of different chemical potential (Killops and Killops, 2005). This process is therefore independent of petroleum bulk flow rates and is of major significance in sedimentary sequences of poor to fair hydrocarbon generation potential (Leythaeuser et al., 1983; Stainforth and Reinders, 1990; Thomas and Clouse 1990 a, b, c).

Mann et al. (1997) concluded that several of the above described processes occur in nature simultaneously or subsequently. Those process might then individually contribute to the composition of the expelled hydrocarbons.

Retention and desorption processes based on different molecular properties (e.g. solubility and polarity), and the porosity evolution of the effected lithologies controlled by kerogen swelling and shrinking are additional factors which control the petroleum composition (Ritter, 2003; Erstas et al., 2006; Kelemen et al., 2006, Han et al., 2015; Han et al., 2017).

1.2.3 Composition of generated hydrocarbons and petroleum

On average, generated petroleum consists of 84% carbon, 13% hydrogen, 1.5% sulphur, 0.5% nitrogen and 0.5% oxygen. In addition, metals, metalloids, alkaline earth metals and non-metals (Si, Fe, Al, Ti, Ca, Mg, V, Mo, Ni, Ba, Sr, Mn, Pb, Cu, Cr, U) have been detected (Pohl and Petrascheck, 2005). The composition of petroleum and generated hydrocarbons varies to a large extend, depending on the source, the depositional environment and secondary alteration processes. In general, the following compound classes are frequently described in petroleum accumulations and produced petroleum.

Paraffins, also known as n-alkanes, are chemical compounds consisting only of carbon and hydrogen atoms. A series of linked carbon atoms is called a carbon skeleton. Paraffins have the chemical formula C_nH_{2n+2}. Economically, the paraffins are the most important compounds, since they can easily be processed into valuable products like gasoline or other distillates (Pohl and Petrascheck, 2005).

Naphtenes or cycloalkanes are chemical compounds consisting of one or more rings of carbon atoms. Similar to paraffins, naphtenes have single bonds (saturated) and consist only of carbon and hydrogen. The general chemical formula for cycloalkanes is $C_nH_{2n(n+1-g)}$ where n is the number of carbon atoms and g is the number of rings in the molecule. Naphtenes build up steroids and terpenes. Cycloalkanes are common components of crude oil, with up to 50 wt.%. Their abundance increases with

increasing density of the crude oil. High concentrations of naphtenes can cause asphaltic residua during the refining process (Pohl and Petrascheck, 2005).

Aromatics are historically named after their characteristic smell. These compounds contain the ring structure of benzene (C_6H_6). Aromatic molecules have at least one ring system with six carbon atoms. The entire molecule is planar, and all bonding angles are 120°. Due to the delocalized π-electrons all six carbon bonds are equal, and it is not possible to distinguish between single and double bonds. Therefore, two mesomeric structural formulas, where single and double bonds alter, are conventionally used. In comparison to non-aromatics, aromatics have a comparably high enthalpy of bonds, which makes the compounds less reactive (Mortimer, 2007).

Asphaltenes consist primarily of carbon, hydrogen, oxygen and nitrogen. They are part of crude oils and rock extracts and reflect the heaviest compound class. The distribution of their molecular masses is in the range of 400 amu – 1500 amu (Pohl and Petrascheck, 2005).

Biomarkers are also known as “geochemical fossils”. Although biomarkers are subjected to chemical transformation and rearrangement processes during the diagenesis stages, it is in some cases possible to related them to their biological precursors (e.g. cell walls of bacteria). Their chemical structure (or rearranged structure) is preserved through the processes of diagenesis and partially through the catagenesis. Many biomarkers initially have functional groups but lose them during diagenesis. Therefore, the products are mainly saturated hydrocarbons, except for functionalized components (e.g. lipid acids), which might survive the diagenesis. Due to hydration of unsaturated hydrocarbons, aliphatic hydrocarbons, such as hopanes and steranes, arise. Instead of hydration, cyclic systems with six carbon atoms and a double bond can be aromatized (e.g. monoaromatic steroids). Petroleum contains a relatively low amount of lipid biomarkers (< 1wt. %), nevertheless they bear information on the source, thermal maturity, migration and biodegradation of a crude oil or rock extract (Killops and Killops, 2005).

1.3 Geological Background of the study area

The research well BH 10-2008 is located on Svalbard (Spitzbergen) which is an archipelago in the north-western region of the Barents Sea. The northern part of Svalbard is partially covered by Palaeozoic sediments, while Mesozoic and Cenozoic rocks are dominating the outcrops in the southern part of Svalbard (Ritzmann et al., 2002).

Two hypotheses of the tectonic evolution of the Central Tertiary Basin (CTB) of Svalbard compete in literature. The first hypothesis suggests that the Paleogene of the Central Basin of Svalbard is subdivided into two tectonic regimes, in which the Paleocene is followed by an Eocene compression (Steel et al., 1981, 1985; Müller & Spielhagen, 1990). Another hypothesis by Bruhns and Steel (2003) and Lüthje (2008) suggests that the CTB originated during the Paleocene as a flexural depression connected to the west Spitsbergen fold and thrust belt. The latter hypothesis has recently been supported by Petersen et al. (2016) through U-Pb age dating of Paleocene and Eocene sandstones in the CTB. The basin shape is asymmetrical leading to a thickening of the Palaeogene sediment deposits towards the south (Livsic 1974; Nøttvedt et al., 1988; Nagy, 2005).

The sedimentary sources for the Paleocene and Eocene sequences in the Central Basin have changed throughout the evolution of the respective sequences. According to Bruhns and Steel (2003) the Paleocene sediments were mainly sourced by the erosion of Mesozoic rocks in the eastern part of Svalbard whereas the Eocene units were fed from the weathering products of Precambrian, Palaeozoic and Mesozoic rocks in western regions.

The central basin fill is comprised of the Lower and Upper Van Mijfjorden Group sediments. The lower part consists of Paleocene sediments comprising the Firkanten, Basilika and Grumantbyen formations. The upper part of the succession consists of the Eocene Frysjaodden, Battfjellet and Aspelintoppen formations (Steel et al., 1985; Manum and Throndsen, 1986 Dallmann et al., 1999). The lowermost Paleocene Firkanten Fm. mainly represents a deltaic and shoreline to prodelta and shelf

depositional environments and is the target of coal mining (Lüthje, 2008; Marshall et al., 2015a, b). A specific focus in several scientific investigations is related to the so-called Paleocene-Eocene Thermal Maximum (PETM) in the CTB (Cui et al., 2011; Dypvik et al., 2011; Nagy et al., 2013). In contrast to other PETM locations, where negative carbon isotopic extrusions (CIE) correlate with elevated organic carbon contents (Sluijs et al., 2006; Stein et al., 2006, Gavrilov et al., 2009; Soliman et al., 2011), the CTB of Svalbard does not show the same features. The deviation from the findings at other localities has been attributed in literature to either high sedimentation rates or a possible reduction in the primary productivity (Cui et al., 2011; Harding et al., 2011).

1.3.1 Research well BH 10 – 2008

Well BH 10-2008 was drilled in 2008 as a cooperation between the Geological Survey of Norway and different industry partners (location see Figure 2). The well has a total depth of 1084.6 m and penetrated Paleocene and Eocene formations of the Tertiary Basin on Svalbard (Figure 3; cf. Grundvåg et al., 2014). The entire sediment successions have been cored and provide exceptional study material of the CTB. The well section was sedimentological interpreted and studied prior to this PhD thesis by Elvebakk et al. (2008), Johannessen et al. (2011), and Grundvåg et al. (2014).

In the following paragraphs, the depth information below refers to meters of measured depth (Figure 3) from the top of the core.

The stratigraphically oldest formation in the well is the Paleocene Basilika Fm. and has been encountered between the end depth of the well at 1084.6 and 930 m and consists of silt- and mudstone. The sediments represent a shelf depositional environment. The Paleocene Grumantbyen Fm. was observed between 930 m and 812 m. The formation represents a highly bioturbated sandstone of shallow marine environments (Øygard, 2016). The base of the Frysjaodden Fm. was assigned to 812 m and with a total thickness of about 640 m the top is reached at 175 m. The lower section of the Frysjaodden Fm. is of Paleocene age. The transition to Eocene strata is marked by a maximum flooding surface at 780 m.

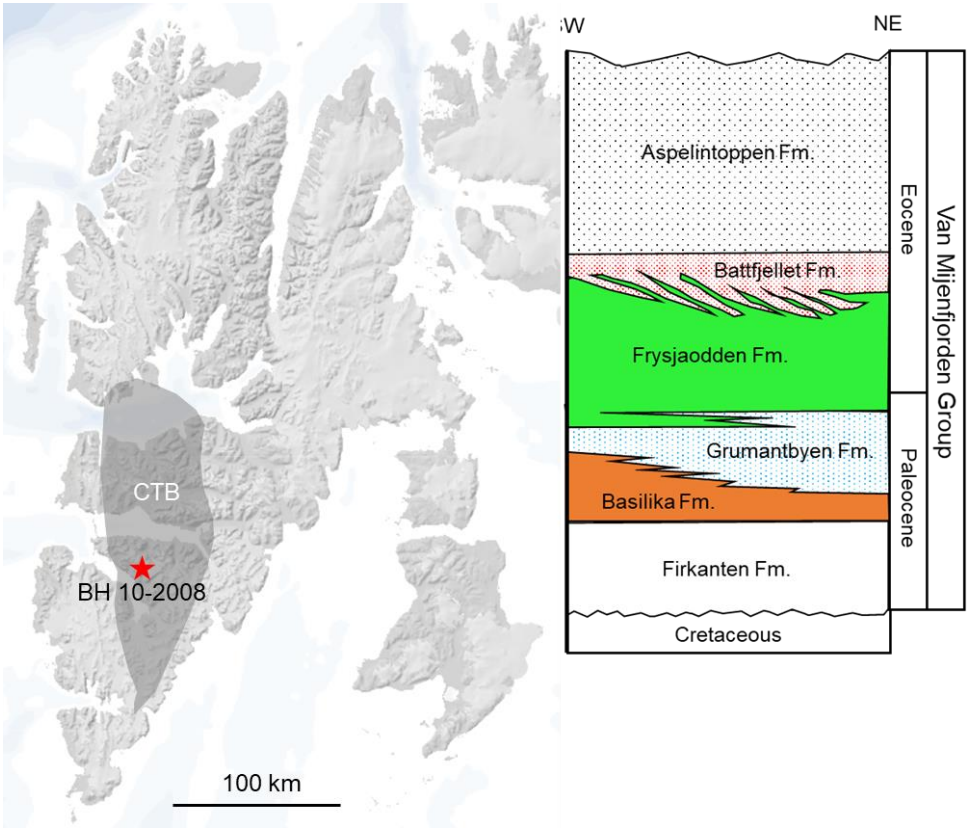

Figure 2: Location of the investigated research well BH 10-2008. The right side contains the stratigraphy of the Van Mijenfjord Group adapted and redrawn from Helland Hansen (1992). The investigated well section reaches a depth of 1084 m within the Paleocene Basilika Fm.

The transition from the Paleocene into the Eocene is interpreted by Cui et al. (2011) and Dypvik et al. (2011) to be related to the so-called Paleocene-Eocene climatic thermal maximum. Those sediments are part of the Frysjaodden Fm. which is a dominant part in the analysed sediments. Sedimentological, the Frysjaodden Fm. is separated into three sections. The lower section consists of silt- and clay-stones which represent open marine depositional conditions. Those marine depositions persist to the base of the Bjørnsonfjellet Mbr. The Bjørnsonfjellet Mbr. is predominantly comprised of sandstones with alternating sequences of shale and siltstone. The lowermost section of the Bjørnsonfjellet Mbr. (above 415 m) is interpreted as a turbidite layer, representing distal basin floor sands. The third and last depositional change within the

Frysjaodden Fm. commences at 330 m and reaches up to 175 m in the well. It consists of siltstone with interbedded thin layers of sandstone. These strata are related to slope depositional conditions. The Eocene Battfjellet Fm. above the Frysjaodden Fm. begins at 175 m and the top is reached at 95 m in BH-10-2008. The formation is dominated by sandstones with interbedded mud- and claystones pointing to shelf edge to deltaic environments. The Eocene Aspelintoppen Fm. is located between 95 m and the top of the well. The formation consists mainly of intervals of alternating sand and shale layers with intercalated coal horizons of up to 30 cm thickness. The depositional condition is interpreted as coastal plain to fluvial-deltaic. The top of the Aspelintoppen Fm. is marked by a glacial erosion surface of recent age.

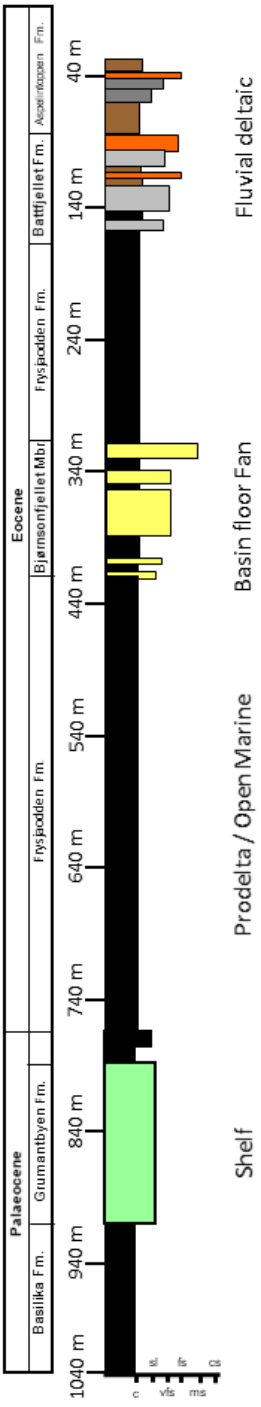

Figure 3: Simplified geological record of the research well BH 10-2008. The formations encountered in the well comprise the Basilika Fm., the Grumantbyen Fm., the Frysjaodden Fm. (including the Bjørnsonfjellet Mbr.), the Battfjellet Fm. and the Aspelintoppen Fm. Note that the Grumantbyen Fm. was not part of the sampling campaign. The lithologies in the Grumantbyen Fm. consist mainly of highly bioturbated, organic lean silt and sandstones. The well has a total depth of 1084 m (mD) with full core recovery. The figure was redrawn after Grundvåg et al., 2014.

2. Scope

Understanding petroleum generation in and migration out of source rocks are important elements in the field of petroleum system analysis. To expand existing concepts into comprehensive geochemical and physical approaches this PhD study is conducted on the topic of primary migration and expulsion of hydrocarbons, using concepts that are based on new observations and measurements derived from the core material of the research well BH 10-2008. The core material used for the presented study has proven to be of exceptional quality in terms of preservation and purity. No contaminating mud additives have been used during the drilling process. The well was drilled with salt water.

The described PhD project focusses on the observational aspects of a little investigated Cenozoic basin on Svalbard comprising the organic matter containing rock depositional environment as well as the state of hydrocarbon generation. This provides the framework in which petroleum expulsion and migration is expected to have happened, but not to an extent that large mass movements occurred. Bulk, molecular and isotopic geochemical parameters were used to attempt a qualitative and quantitative description of hydrocarbon migration of the organic rich layers. The aims of this study can be subdivided as follows:

1. Investigation of new geochemical methodologies that might help to improve the understanding of molecular and isotopic processes in organic geochemistry.

2. Description and evaluation of depositional environments of organic-rich rocks including kerogen characterization and possible sulphate reduction influences.

3. Description of the thermal maturity of the research well, with special focus on the difference between molecular maturity markers in the bitumen and kerogen maturity.

4. Evaluation and description of molecular fractionation effects of compound classes and compounds (i.e. selected biomarkers and light hydrocarbons) including potential isotopic fractionation effects.

5. Evaluation and description of concentration gradients of compound classes and selected molecular species within source rocks and adjacent rocks.

6. Creating a synoptic concept of primary migration and expulsion based on project data integrated into existing knowledge.

3. Methods and Material

3.1 Outline

The following chapter summarises the organic and inorganic geochemical methods that were used for this study. Method developments that were part of a dedicated research paper are described in the respective section of this thesis book (Paper I and Paper III).

All chemicals used for the presented study were of high analytical grade (HPLC grade solvents). All reference and calibration materials have been purchased from certified institutions. For more details, the reader is referred to the specific manuscripts.

All analyses that were performed were quality controlled by repeated analyses of NSO-1, JR-1 and SR-1 reference material as described in the Norwegian Industry Guide to Organic Geochemical Analyses (Weiss et al., 2000).

3.2 Sampling

Sampling was done in the core repository of Equinor ASA in Bergen. The 1083.6 m long half core of well BH 10 - 2008 was sampled based on visual and sedimentological properties as well as based on the results of a pre-screening campaign. In sections of optical homogeneous shales, a sampling interval of < 4 m was maintained. The organic lean Grumantbyen Fm. has been excluded from the sampling. In total 218 samples were taken from the core section and analysed.

3.3 Sample preparation

It was determined that the sample material was not affected by drilling mud contamination. The research well has been drilled with salt water as the only additive. Therefore, no special treatment for drill mud contamination was performed.

All samples were crushed to analytical fine grade with a pestle and mortar prior to analysis.

3.4 Organic geochemical analysis

3.4.1 Solvent extraction and asphaltene precipitaion

The extraction of sediment samples was done with a Soxtec 2050. The amount of sample material subjected to solvent extraction was determined by the Rock-Eval S1 value. For the sample material from BH 10-2008 between 15 g and 60 g of sediment sample have been extracted. The extraction was accomplished with an azeotropic mixture of dichloromethane (DCM) and methanol in a ratio of 97:3 (v:v). Reduced copper wires were added to the solvent mixture in order to remove free sulphur from the extracts and prevent boiling retardation. The extraction was carried out at 165 °C for 4 hours. After the extraction process was completed, the extracts were centrifuged for 5 minutes to settle remaining sediment particles. The supernatant was collected, and an aliquot was dried and weighed to calculate the extract yield. An internal standard containing both saturated and aromatic compounds, was added to the mixture. The extracts were concentrated using a gentle stream of N_2.

The asphaltenes were precipitated by adding approximately 40 times the volume of the concentrated extracts of cold n-pentane. The mixture was placed in a dark room for 8 h until the precipitation was completed. The asphaltene content was quantified by weight.

3.4.2 Group type separation (MPLC)

The separation of the internal standard spiked extracts into saturated, aromatic and NSO (nitrogen, sulphur and oxygen) containing fractions was done on an HP 1100 series HPLC system connected to an automated fraction collector. The main column used for the separation of the compounds classes was a Lichroprep Si 60 (40 – 63 pm), preparative HPLC column. A column containing preconditioned Kieselgel 100 was used as precolumn. A detailed description of the analytical setup is given in Radke et al. (1980).

3.4.3 TLC-FID analyses (IATROCScan)

The distribution of saturated, aromatic and NSO compounds was determined by thin-layer chromatography flame ionization detector (TLC-FID). An aliquot of the maltene fraction was concentrated to approximately 15 mg extract / ml solvent. Pre-cleaned Chromarods were spotted with 30 µg of the maltene fraction approximately 2.5 cm above the lowermost end of the Chromarod. A gentle stream of N_2 was used to remove excess solvent. After the solvent was dried off, the Chromarods were placed into an n-hexane bath (30 minutes for elution of saturates), followed by a toluene bath (10 minutes, elution of aromatic compounds). The last bath contained a mixture of 97:3 (v:v) DCM and methanol (3 minutes for the elution of NSO compounds). After the rods have been dried in an oven at 60 °C for 5 minutes, the Chromarods were placed into the IATROSCAN where the amounts of the different fractions were determined by flame ionization detection.

3.4.4 Rock-Eval

The sample material investigated in this PhD study was analysed with a Rock-Eval 6 analyser. A subsample set was analysed before and after extraction. In addition to the standard Rock-Eval bulk method (Behar et al., 2001) all samples were analysed with the so-called "Rock-Eval shale method" as proposed by Romero-Sarmiento et al., 2016. This specific method is supposed to support differentiation between the free and adsorbed/refractory hydrocarbons in the sample material by reducing the Rock-Eval crucible insertion temperature to 100 °C and introducing a second heating phase into the standard Rock-Eval program from 200 °C to 350 °C. The latter temperature is 50 °C higher than in the Rock-Eval bulk method. The results from the Rock-Eval shale method are suggested to be more realistic in terms of comparability to conventional solvent extraction yields (Romero-Sarmiento et al., 2016). All data on S1, S2, TOC and HI are given in the typical standard parameterization (cf. Behar et al., 2001).

3.4.5 Elemental analysis coupled isotope ratio mass spectrometry (EA-IRMS)

To determine the carbon, nitrogen and sulfur content as well as the carbon isotopic composition of the total organic carbon ($\delta^{13}C_{TOC}$) an Elementar Vario

Pyrocube operated in CNS (carbon, nitrogen and sulfur) mode was used. The combustion temperature was set to 1120 °C, the reduction tube was operated at 850 °C. The Pyrocube was connected to an Isoprime 100 IRMS (isotopic ratio mass spectrometer).

For elemental analyses, 1 to 10 mg of the sediment sample was put into pre-extracted tin capsules. For the determination of the TOC and for the measurement of the isotopic composition, the samples were inserted into silver capsules. Carbonate minerals contained in the sample material, was removed through fumigation with hydrochloric acid (HCl) for 4 hours.

The stable isotope composition of carbon is reported in delta (δ) units as the per mil deviation (‰) of the isotopic ratio relative to a known standard:

$$\delta = \frac{R_{Sample} - R_{Standard}}{R_{Standard}} \times 1000$$

where R is the ratio of $^{13}C/^{12}C$. All measurements were normalized to Vienna Pee Dee Belemnite (V-PDB) standard.

3.4.6 GC-FID-MS

Analyses of saturated and aromatic hydrocarbons were carried out on a two column GC-MS-FID system. The instrument consists of an Agilent 6890 GC combined with a flame ionization detector (FID) and a mass selective detector (MSD), Agilent 5973N. The oven is equipped with two chromatographic columns, of which the first column is connected to the FID. This column was an Agilent DB-1 capillary column (length 20 m, inner diameter 0.1 mm, film thickness 0.2 um). The second column was connected to the MSD. The MSD column was an Agilent Ultra-1 (for aromatic fractions HP-5 MS of the same dimensions) capillary column (length 50 m, inner diameter 0.2 mm, film thickness 0.33 um). Helium was used as the carrier gas. The GC oven was programmed with an initial temperature of 70 ºC (hold for 2 minutes), afterwards the temperature was increased to 150 ºC at a rate of 5 ºC/min. Finally, the

temperature was increased to 325 ºC at a rate of 2 ºC/min. The final temperature was held for 15 minutes.

The MSD was operated in ion impact ionization mode (EI) at 70 eV. The source temperature was set to 230 ºC, the quadrupole temperature was set to 150 ºC.

Major straight chain and branched alkanes were quantified with the signal generated from the FID. Trace compounds such as saturated biomarkers, as well as aromatic compounds were measured and quantified using the MSD in single ion monitoring mode (SIM).

3.5 Inorganic geochemical analyses

3.5.1 XRF

The sample material was ignited at 1000 ºC and the loss of ignition was determined by weight. The ignited powders were fused with $Li_2B_4O_7$ in a Classie-Fluxy instrument to make glassy beads.

Major elements (Al, Ca, Fe, K, and Si) were measured using a Bruker S4 Pioneer X-ray fluorescence spectrometer (XRF). The quantification for the measured elements was achieved by external calibration curved produced from certified standard materials. The quality control is based on the measurement of USGS CRM BCR2 (Basalt, Columbia River) standard.

3.5.2 ICP-MS

For inductively coupled plasma (ICP) coupled to a mass spectrometer (MS) analyses, the analytical fine sample powders were ignited at 1000 ºC to remove the organic carbon contained in the sample material. The sample was afterwards digested in a mixture of HNO_3 and HF in a Savillex beaker on a heater plate at 135 ºC. The generated, dried solution was diluted in 2N HNO_3. Aqua regia (HNO_3 /HCl, 1:3, v:v) was used in order to remove undissolved oxides. Finally, the concentration of the sample solution was adjusted with HNO_3.

The concentration of trace elements (Ba, Co, Cr, Cs, Cu, Mn, Nb, Ni, Pb, Rb, Sc, Sr, Th, Ti, U, V, Y, Zn, Zr, Ga, Mo and the Rare Earth Elements) was measured using a Thermo Scientific Element XR High Resolution ICP-MS. External calibration curves were produced with multi-element standard solutions prepared from certified single element solutions. The quality control is based on the measurement of USGS CRM BCR2 (Basalt, Columbia River) standard.

3.5.3 QEMSCAN

Quantitative Evaluation of Minerals by Scanning Electron Microscopy (QEMSCAN) was performed with a Quanta FEG 650 F scanning electron microscope equipped with two Bruker XFlash 5030 energy dispersive detectors (EDS). All analyses were performed on selected thin section at 15 kV accelerating voltage and a specimen current of 10 nA. For better conductivity, carbon coating was applied to the thin sections. The results for major minerals have been verified with additional X-ray diffraction (XRD) measurements.

4. Main Results

4.1 Outline

The following chapter summarizes the aim, execution, and major findings that are described in detail in each of the included publications and manuscripts. Five individual manuscripts have been prepared in the course of the thesis project. Two of the manuscripts are published in peer-reviewed journals (Paper I and Paper III). The remaining manuscripts have been submitted in 2019 to international journals and were under review at the point the thesis has been submitted.

4.2 Paper I - Organic geochemical research analytics of the petroleum industry - Enhanced data density and method flexibility using gas chromatograph multiple detector coupling

Aim: The aim of the first publication was to introduce a new combination of analytical instruments in order to enhance the methodological productivity and data density per sample. The concept was to use a set of different detectors and couple them to one gas chromatographic system and two multi-purpose samplers to be able to analyse multiple sample matrices on a single system and detect and measure different compounds and the carbon isotopic composition simultaneously.

Execution: A single gas chromatograph was connected to a quadrupole time of flight mass spectrometer (Q-TOF), a combustion furnace, an isotopic ratio mass spectrometer (IRMS), a thermal conductivity detector, and a flame ionization detector (FID). By using two columns of which one was a Pora Plot Q in a low thermal mass oven (LTM) and a DB-1 it was possible to use the instrument for gases as well as liquid samples. The sample split between the different detectors was adjusted by a single four port splitter. The split ratio was set by flow restriction. In order to prevent solvent peaks from entering the combustion furnace a vent system (pressure operated) was developed. Commercially available vent options conduct the solvent peak into the FID detector which disables the detector during IRMS analyses. The customized vent

option was used to operate all detectors simultaneously. A schematic of the developed system is displayed in Figure 4.

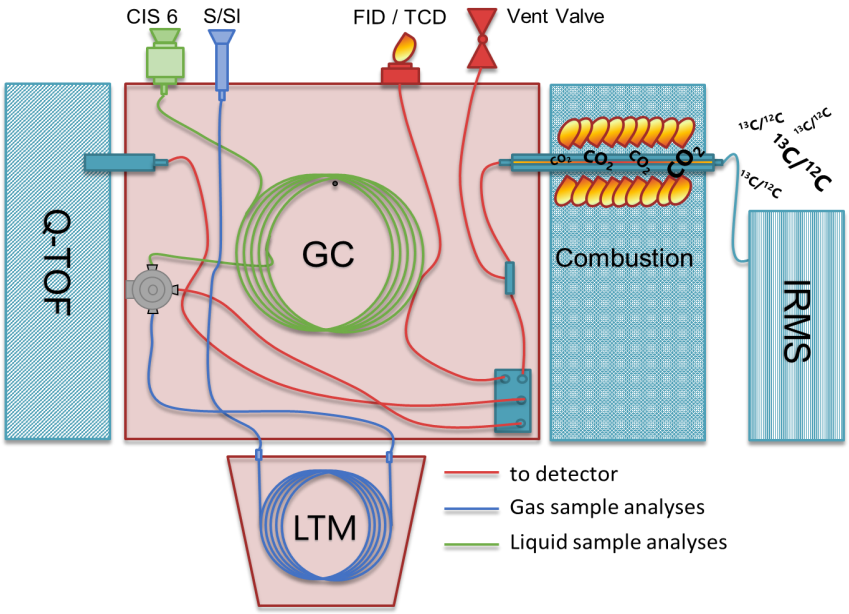

Figure 4: Schematic drawing of the developed analytical system. Red lines are capillaries that divert the sample into the detector systems. Blue lines indicate the flow path for gas samples, green lines indicate the flow path for liquid samples (picture from Doerner et al., 2018).

Findings: The system was tested using different gas and liquid standards (NGS reference gas samples and NSO-1 standard oil). It hereby was demonstrated that advanced liquid and gas analyses could be performed with the newly developed combination of instruments/detectors. In addition, it was shown, that compound specific isotope analyses of straight chain alkanes and branched alkanes can be performed simultaneously with high resolution mass spectrometry without having to inject large volumes (Figure 5). Since the Q-TOF system was always operated in full scan mode, the full structural information of individual compounds (e.g. biomarkers) was maintained.

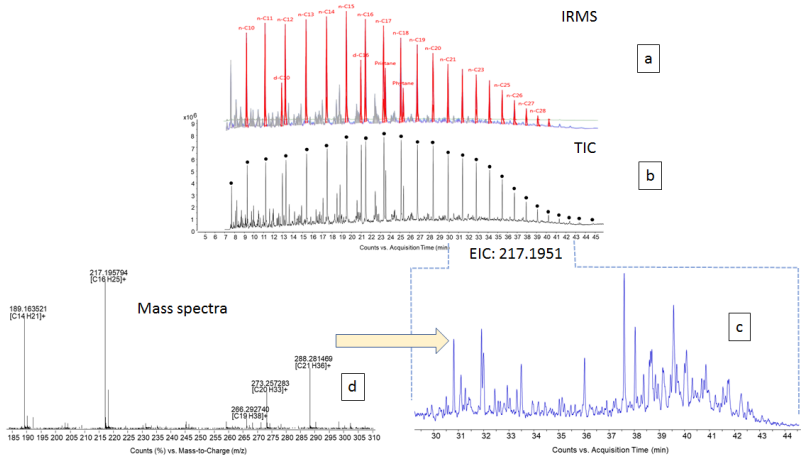

Figure 5a-d: General data that has been generated with a single injection of the saturated NSO-1 fraction. a: The IRMS record for the compound specific isotope measurements of n- and i-alkanes. b: High resolution mass spectrometry generated from the Q-TOF detector. c: Extracted ion chromatogram for m/z 217.1951 ± 10 ppm, showing the steranes. d: Mass spectrum of a selected sterane (background subtracted) and elemental composition calculation for each fragment with Agilent Qualitative analysis software (Figure from Doerner et al., 2018).

It was found that the separation of the different sample flow lines helps to reduce the effects of cross contamination. The latter can cause severe problems especially if gas samples and liquid samples are passed through the same flow path.

Multiple injections with standard and reference materials confirmed that both, accuracy and precision of the FID, TCD, and IRMS system are suitable to measure the molecular and isotopic composition of gas samples realistically. By using the multi-purpose sampler in combination with an Isotube® rig, the sample preparation for gas sample analyses could be reduced to a minimum. It was demonstrated that the changes to the sample/split ratio between the different detectors introduced by temperature changes in the GC oven can be neglected. Slight changes in the sample split were compensated through the measurement of the sample peaks against the internal standard mixture.

The different detector systems require the use of two computer systems simultaneously for the data acquisition as well as three software packages. Although

the different software suits were interconnected, it was noticed that the performed analyses need to be monitored more frequently when compared to single purpose (stand-alone) instruments. The complexity of the system made it also more challenging to troubleshoot in cases of analytical failures which potentially can lead to increased downtimes of the complex system.

The generated reference dataset in this study served as a quality control and guideline through the other studies that were conducted within this PhD project.

4.3 Paper II - Geochemical characterization of the depositional environment of Paleocene and Eocene sediments of the Tertiary Central Basin of Svalbard

Aim: The negative carbon isotopic excursion occurring within the Paleocene Eocene Thermal Maximum (PETM) on Svalbard has been established in several studies and was related to specific environmental conditions that were present during that time (e.g. Cui et al., 2011; Harding et al., 2011). In contrast to other PETM locations (Sluijs et al. 2006; Stein et al. 2006; Gavrilov et al. 2009; Soliman et al. 2011), the Central Tertiary Basin PETM sediments show no elevated organic carbon concentrations. Therefore, the aim of this study was to elucidate the reasons for the low concentration of organic carbon within the Paleocene Eocene transition.

The present record of the CTB sediments with an organic and inorganic dataset and related interpretation of the depositional conditions should be expanded. The generated data and interpretations regarding the depositional condition of the investigated research well are the basis for advanced organic geochemical interpretations.

Execution: 218 samples from the well BH 10-2008 have been selected for organic and inorganic geochemical analyses. The methods that were used for this study comprised elemental analyses (EA) providing the concentrations of carbon, nitrogen and sulfur, major and minor elements using X-ray fluorescence (XRF), and inductive coupled plasma mass spectrometry (ICP-MS). In addition, carbon isotopic measurements on the total organic carbon were performed using an EA-IRMS instrument coupling. Thin sections were prepared on a subsample set for quantitative evaluation of minerals by scanning (QEMSCAN).

Findings: The integration of the measured data into the general depositional concepts of the CTB helped to better evaluate, understand and describe the depositional conditions in the area of the investigated well. The Paleocene and Eocene succession consist mainly of siliciclastic rocks with minor carbonate contributions. The

depositional reconstruction for the different formations supports findings from earlier studies of the CTB at different locations.

The primary productivity was elevated during the Paleocene Eocene transition mainly driven by elevated rates of weathering, enhanced run off and consequently a higher nutrient supply. This is reflected in the K/Al elemental ratio in combination with total concentrations of Cu and Ni. Interestingly, the proposed elevated primary productivity is not fully preserved in the measured TOC of the sediments. Microbially induced sulfate reduction had a strong impact on the preservation of the organic matter in the sediments during the Paleocene Eocene transition. It was possible to estimate the original organic carbon concentration of the sediments before microbial sulfate reduction, by using published equations to quantify this process (Lallier-Vergès et al., 1993; Vetö et al., 1994; Lückge et al., 1999). The results show that the original TOC was up to two times higher than the preserved concentration (Figure 6).

The differentiation between marine versus land plant material input into the CTB was determined through the introduction of a C/N ratio endmember calculation. It was shown that the organic matter within the Basilika Fm. and the Frysjaodden Fm. consist mainly of marine organic matter. The younger Battfjellet Fm. and Aspelintoppen Fm. contain higher proportions of higher land plant material.

The original isotopic composition of the organic matter prior to microbial degradation was estimated by combining the restored loss of the original organic carbon through sulfate reduction, the contribution of marine versus terrestrial organic matter and the measured $\delta^{13}C_{TOC}$. A Rayleigh-fractionation calculation with an assumed fractionation factor of $\alpha = 1.0025$ was used.

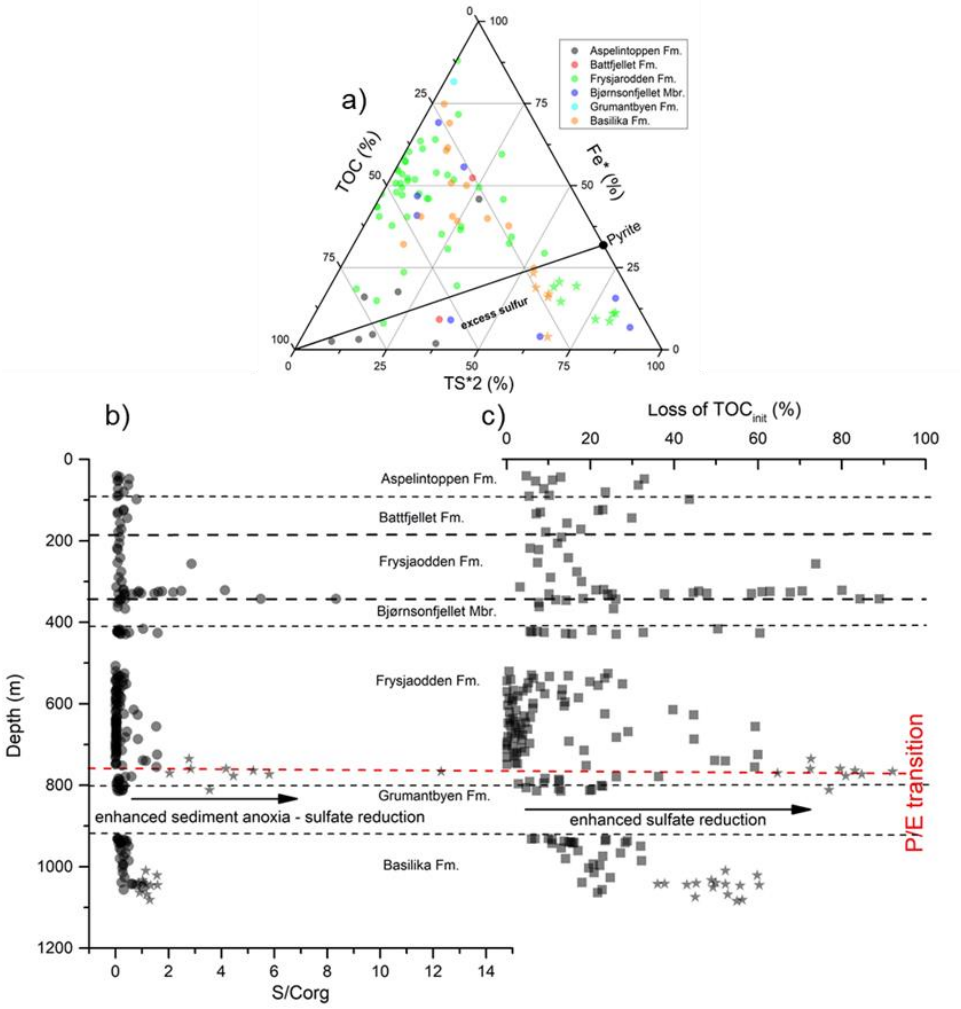

Figure 6a-c: a: Ternary plot of the total sulfur, TOC and reactive iron system (Fe*), the pyrite line is indicating by the solid black line. b: Total sulfur/TOC ratio versus depth, indication changes in the oxygen supply during the Paleocene Eocene transition. c: loss of organic carbon induced by sulfate reduction versus depth, indicating that the loss of TOC was elevated during the Paleocene Eocene transition (Figure from Doerner et al., 2019, under review).

4.4 Paper III - Carbon isotopic analysis of reactive organic matter using a new pyrolysis-cryotrapping-isotope ratio mass spectrometry method: The isotope variation of organic matter within the S1 and S2 peaks of Rock-Eval

Aim: Rock-Eval analyses are frequently conducted in petroleum and organic geochemistry research, but only limited knowledge regarding the isotopic composition of the standard Rock-Eval parameters is present. The presented methodology is created to monitor continuously the isotopic composition of the products generated during a Rock-Eval open-system pyrolysis. The proposed methodology supports investigations of the carbon isotopic fractionation of organic matter induced by thermal maturation. The results improve the understanding of the isotopic composition and differences between mature source rocks and expelled petroleum.

In paper II we found that the impact of sulphate reduction was severe in the sedimentary sequences of the Paleocene Eocene transition. The proposed methodology might help to elucidate the effects of microbial degradation on the carbon isotopic composition of the reactive organic matter contained in respective sample material.

Execution: The GC system described in paper I was equipped with a pyrolyzer unit. The chromatographic column was replaced with a fused silica transfer line without coating. Sediment samples were loaded into quartz tubes and pyrolyzed with the standard Rock-Eval compatible temperature program. A cryotrap was positioned between the combustion furnace and the IRMS detector. With this setup it was possible to monitor the composition of the S1 and S2 peaks generated during Rock-Eval pyrolysis. The S2 peak was monitored continuously, for each 15 ºC of temperature increase during the kerogen pyrolysis. The cryo-trap assured precision and accuracy of the measurements as it helped to focus each single peak for the IRMS measurement as shown in Figure 7.

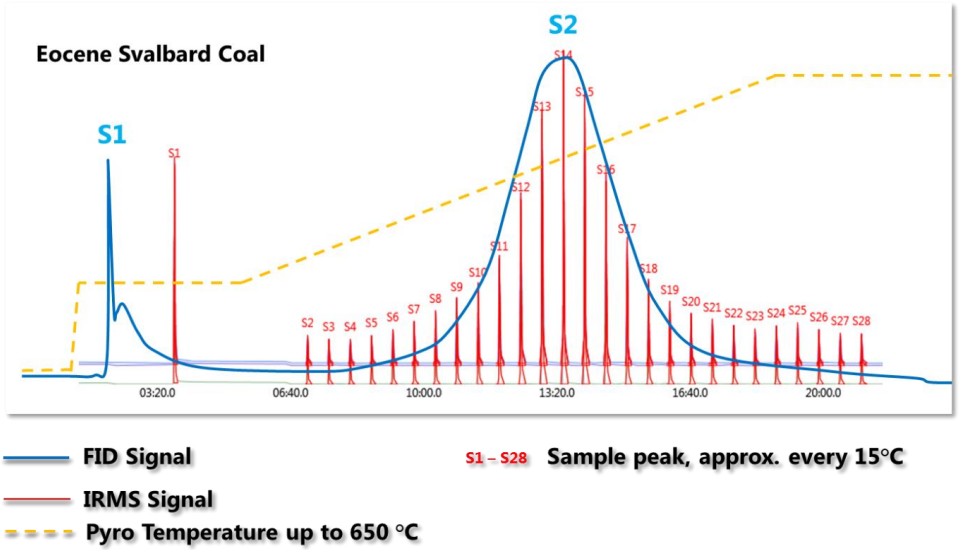

Figure 7: Chromatographic results for the pyrolysis IRMS method. The FID signal is represented by the blue line, the IRMS signal is displayed as red peaks. Both signals were recorded simultaneously (Figure adapted from Doerner et al., 2019).

The sample suite that has been used for this study was comprised of five sediment samples from the well BH 10-2008 covering the Paleocene Eocene transition. In addition, five samples from extensively studied areas (Mahogany Shale section of the Green River Fm. (Western USA), Messel Fm. (Southern Germany), Botneheia Fm. (Svalbard), the so-called Jet Rock of the Whitby Mudstone Fm. (United Kingdom), and Wealden Fm. (Dorset, United Kingdome) were included. The sample material was used to apply the method to sediments originating from a broad range of well-studied depositional settings and thereby helping to set the new datatype into an already studied context.

The method was validated with several certified isotopic standards. No instrumental related isotopic fractionation was observed.

Findings: The new pyrolysis IRMS method allows to measure the carbon isotopic composition of the reactive (pyrolysable) fraction of the organic matter of a sediment sample and monitor its evolution as a function of increasing thermal stress.

The isotopic fractionation occurring during the pyrolysis of the S2 proportion of the individual samples differed significantly. By combining the observed isotopic fractionations with elemental analyses, bulk isotopic analyses, and Rock-Eval analyses, interpretations regarding the preservation state and depositional conditions of the individual samples were suggested (Figure 8).

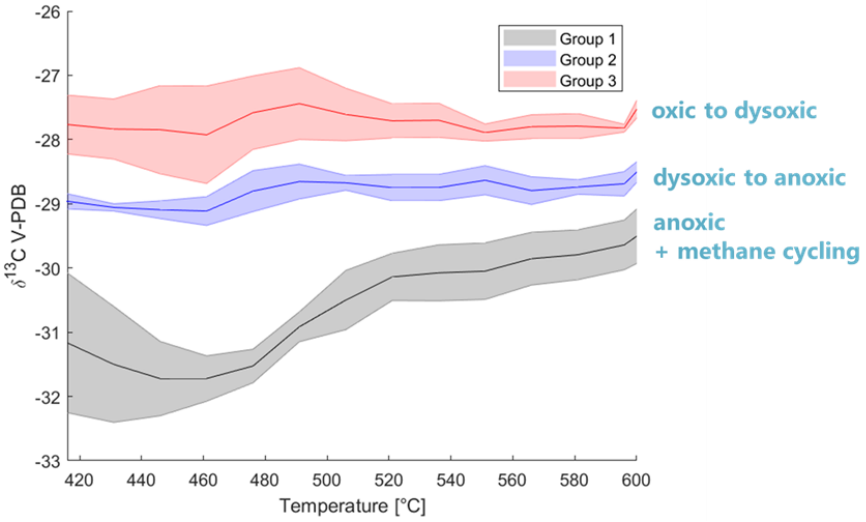

Figure 8: Pyrolysis temperature in ºC versus δ13C values of the pyrolysates (only S2 proportion). The isotopic values exhibit a clustering into 3 groups. The solid lines indicate the average of the isotopic composition of the individual groups, shaded areas show the isotopic variation within each group. All groups are labeled with the depositional condition under which they were deposited (adapted from Doerner et al., 2019).

It was demonstrated that a better state of organic matter preservation is associated with enhanced S2 isotopic fractionation during the pyrolysis experiments. This effect is most likely related to the preservation of the original ^{12}C pool contained in the organic matter, that is less affected by microbial processes during the deposition. In those cases, an isotopic fractionation of up to 3 ‰ was recorded. The sample material from the Paleocene Eocene transition from the study well exhibited a comparably heavy isotopic signature of the reactive organic matter, especially when compared with the isotopic composition of the TOC. Those findings support the severe effect that microbial reworking (e.g. sulphate reduction) had on the sedimentary organic matter in

the Paleocene Eocene transition. The results point towards a preferential consumption of the reactive organic matter proportion during the microbial consumption, which is demonstrated by a depletion of ^{12}C of the reactive organic matter of those sediments.

Although the data set that was presented in the study is not comprehensive, it was possible to establish a maturity driven relationship between the isotopic composition of the S1 and the S2 proportion of the generated pyrolysates. The isotopic difference between the S1 and the S2 approximates each other until peak oil maturities at approximately 0.9 % Vr_{eq} are reached (Figure 9). Samples that plot outside the proposed maturity trend are most likely affected by secondary processes such as biodegradation or staining with bitumen from other sources than from the sample itself.

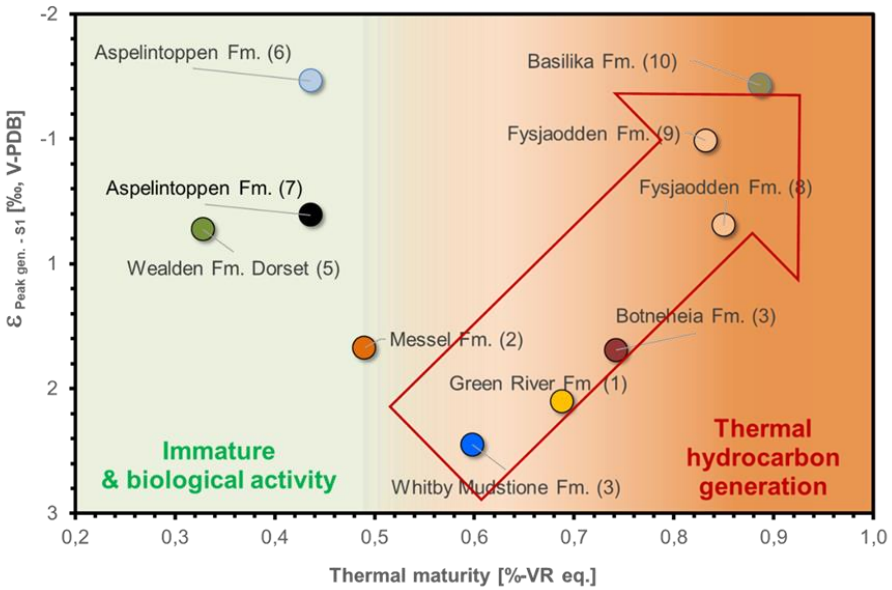

Figure 9: Maturity deduced from the difference of the S2 versus the S1 isotopic composition ($\varepsilon_{Peak\text{-}gen\text{-}S1}$) plotted against the Vr_{eq} calculated from Rock-Eval T_{max}. The green shaded area marks the field of samples that do not follow the maturity trend represented by the red arrow. Those samples are likely affected by secondary processes. Once oil expulsion and primary migration commence, the $\varepsilon_{Peak\text{-}gen\text{-}S1}$ can be used as maturity indicator, assuming that the S1 proportion is generated exclusively from the S2 proportion of the respective sample material (adapted from Doerner et al., 2019).

4.5 Paper IV - Qualitative evaluation of molecular maturity markers in thermally mature sediments, a case study from Svalbard

Aim: The aim of the presented paper is to evaluate the thermal maturity of the investigated research well BH 10-2008. Molecular maturity biomarkers and their different responses to thermal maturity were subject of the investigation. Of special interest was to elucidate on the difference in the maturity trends that can be established by molecular maturity proxies and the kerogen maturity represented by Rock-Eval Tmax measurements.

Execution: 218 Rock-Eval measurements results were compared with the molecular composition of 87 sediment extracts. 47 individual maturity ratios and proxies were investigated and subjected to multivariate statistics. Depth trends of measured maturity parameters and proxies were compared to those of typical facies parameters such as $\delta^{13}C_{TOC}$, total sulphur (TS), atomic organic carbon over nitrogen ratio (C/N), and Pristane/Phytane ratios (Pr/Ph). This supports the identification of maturity proxies that respond mainly to facies changes and those that are most responsive to thermal maturity (Figure 10).

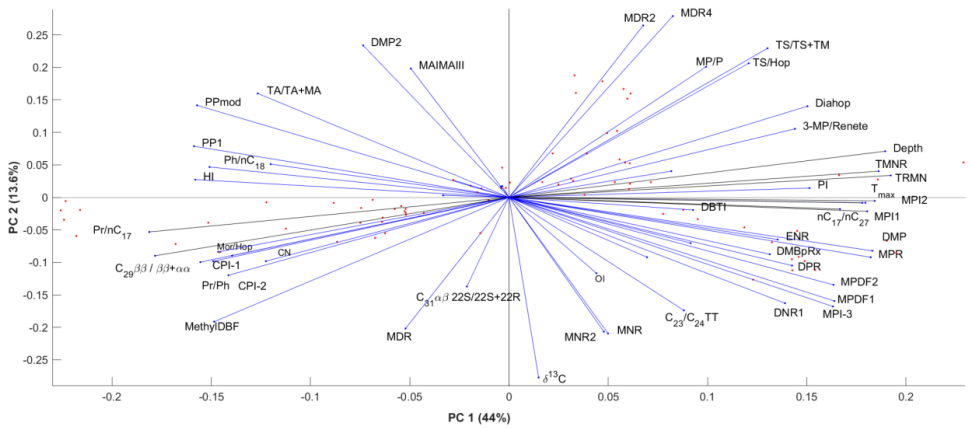

Figure 10: Principal component analyses of maturity and facies parameters. Parameters that exhibit a degree of correlation with depth (maturity) are indicated as black lines. Small angels between the different parameter vectors are indicative for a high degree of correlation, angels of 180 ° are indicative

for counter correlation, e.g. HI decrease with well depth due to hydrocarbon generation (adapted from Doerner et al., 2019; submitted manuscript).

Findings: The investigated well reaches the main oil window at a depth of approximately 780 m, which corresponds to a vitrinite reflectance equivalent of 0.8 % Vr_{eq}.

A set of seven molecular maturity proxies was identified that showed the best correlation with depth and the least response to facies changes, expressed in a correlation coefficient of $r^2 > 0.7$. The most suitable parameters for the study well were MPI-1, MPI-2, DMN, TrMN, C_{29} (ββ/αα+ββ), Pr/nC_{17}, and TMNr.

In addition, a formula was developed that uses the most responsive maturity proxies and combines them in a correlation coefficient weighted, unitless maturity trend, in which parameters that exhibit the highest correlation coefficient get the most weight. The unitless biomarker maturity trend shows a different slope in the maturity trend when compared to the kerogen maturity (Figure 11). It was therefore found that the kerogen maturity trend in the investigated well is to some extend decoupled from the molecular or liquid maturity trend.

We demonstrated that even well correlated parameters (e.g. MPI-1) are affected by other processes than maturity such as facies changes and solubility differences of the compounds incorporated in the MPI-1 calculation, in the kerogen network as described by Ritter (2003). Nevertheless, the proposed unitless biomarker maturity trend might provide a more reliable parameter especially in oil to source correlation, and in cases where it is possible to calibrate the biomarker maturity indicators in the source rock section.

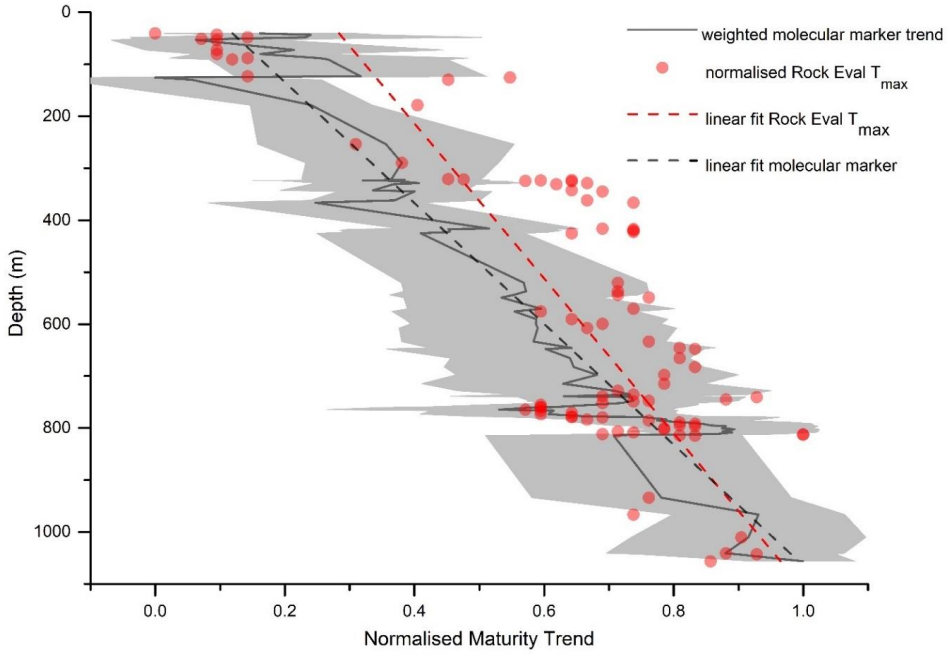

Figure 11: Normalized maturity trend for the combined maturity proxies, consisting of the 7 parameters that exhibit the highest degree of correlation with depth and normalized kerogen maturity represented by T_{max}. Note that the slopes of both trends are different, with the Tmax trend been steeper (adapted from Doerner et al., 2019; submitted manuscript).

4.6 Paper V - Organic geochemical characterisation of hydrocarbon generation and migration at the Paleocene-Eocene transition on Svalbard

Aim: The study described in paper II has shown that the interval prior to the onset of the Paleocene Eocene negative carbon isotopic excursion contains relatively elevated concentration of organic carbon of up to 3 %. In paper IV it was demonstrated that this interval is thermally mature and has reached the peak oil window. The focus of this study was therefore to investigate the hydrocarbon generation potential as well as expulsion induced molecular fractionation effects of the extended Paleocene Eocene transition sequences.

The calculation of the initial potential of a hydrocarbon generating rock sequence and the estimation of the amounts of hydrocarbons that migrated out of those organic rich layers are dependent on the use of realistic measurements regarding the present-day hydrocarbon content. Therefore, three different methods (solvent extraction, Rock-Eval S1 and Rock-Eval Shale method®) are compared in order to use the most realistic data for a back-calculation approach in which the amount of generated, expelled and migrated hydrocarbons should be determined.

Execution: A combination of organic geochemical bulk parameters comprising Rock-Eval analyses, the Rock-Eval shale method, TLC-FID and molecular analyses of selected aromatic and saturated compound was used to investigate potential expulsion induced fractionation.

In order to back-calculate the initial potential of the investigated sedimentary sequences and to quantify the amounts of hydrocarbons that migrated out the sedimentary section enriched in organic carbon, a back-calculation approach originally proposed by Banerjee et al. (1998) was modified and extended. In this approach the C/N endmember calculation introduced in paper II was applied to elucidate on the kerogen composition of the evaluated sample material. For each samples a transformation ratio of the mixed kerogen (mix between kerogen Type II and Type III) was calculated, and the initial hydrocarbon potential was subsequently determined.

Findings: We demonstrated that the standard Rock-Eval S1 data underrepresents the bitumen content in the respective study area when compared with solvent extraction and the Rock-Eval shale method. The results presented in this paper show that the solvent extraction is the most reliable and realistic parameter regarding the total bitumen content of a sedimentary sequence. Based on the presented results it might be possible to calibrate standard Rock-Eval results and the more advance Rock-Eval shale method results to solvent extraction yields and therefore reduce the need for expensive and time intensive solvent extraction.

The investigated well can be subdivided in two sections, a lower organic rich expelling section (source), approximately at 780 m, and an upper receiving (sink) part in which hydrocarbons have been migrating into. As shown in Figure 12 the upper section is enriched in saturated compounds, while the lower source section contains elevated concentrations of asphaltenes and polar compounds, which are preferentially retained in the lower, organic rich section.

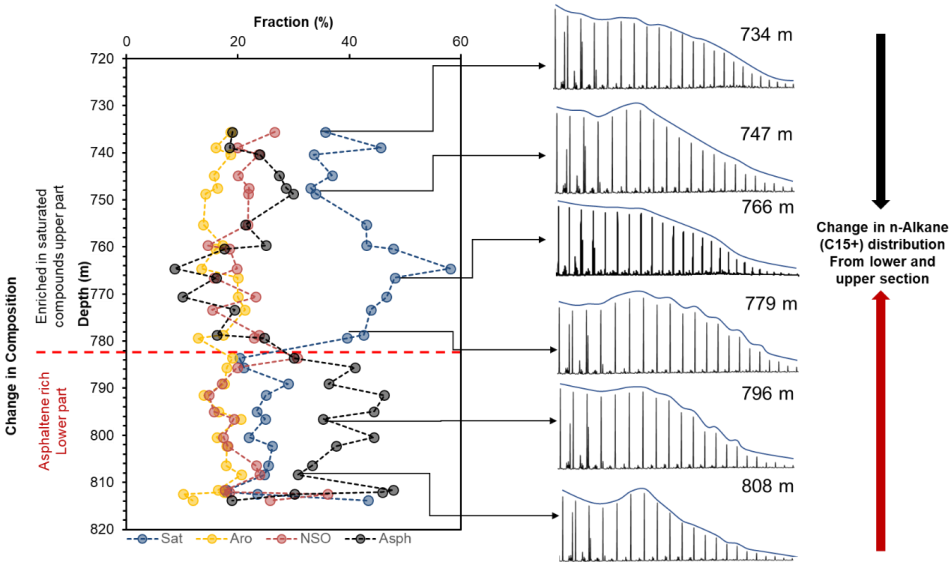

Figure 12: Distribution of the different compound class fractions in the investigated section (saturated, aromatic and NSO compounds). The distribution of n-alkanes is represented by the chromatograms on the right (adapted from Doerner et al., 2020, submitted).

The application of the kerogen mixing back-calculation approach to restore the original hydrocarbon potential and subsequent calculation of the amount of migrated hydrocarbons provided a realistic outcome when extraction yield and extracted $S2_{ex}$ data was used instead of the standard Rock-Eval S1 and S2. The back-calculation performed with standard Rock-Eval S1 and S2 data overestimated the migration loss and did not result in a hydrocarbon sink in the upper core section, which was indicate by molecular and bulk analyses (Figure 13).

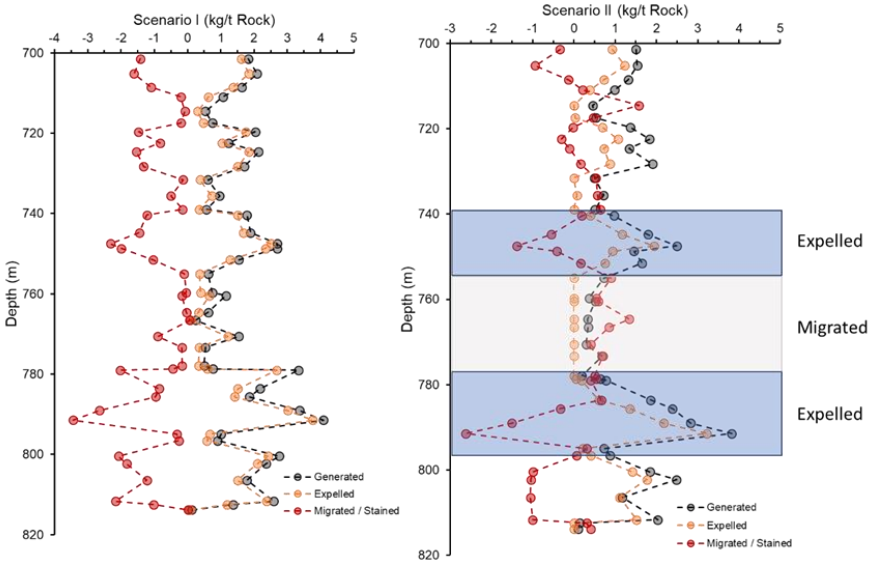

Figure 13: Results from the modified back-calculation approach after Banerjee et al., 1998. Scenario I was calculated with standard Rock-Eval parameters (S1 and S2) while Scenario II was calculated with extract yield and $S2_{ex}$ (adapted from Doerner et al., 2020, submitted).

5. Concluding remarks and further work

5.1 Condensed conclusion

The presented PhD study is divided into two parts. The first part of the study is dealing with the development of new analytical methodologies that support geochemical interpretations and data generation. In paper I a new analytical system was introduced that used multiple advanced detectors coupled to a single gas chromatograph in order to enhance the data density per sample injection. The flexibility of the system in combination with a high level of automation are key features in a research field that is steadily increasing in its dependence on high amounts of high-quality data, especially when advanced technologies such as artificial intelligence and machine learning shall be implemented.

The second method development is presented in paper III. The paper describes for the first time an online measurement technique measuring the isotopic composition of the Rock-Eval S1 and S2 comparable pyrolysates fractions. Although the described study contains only limited data, the preservation of organic matter could be tied to its specific isotopic fractionation behaviour. The rapid heating rates applied to the sample material are not mimicking natural condition, but the results give rise to the assumption that isotopic fractionation between the kerogen and the produced liquids is occurring in natural system as well. The proposed analytical setup helps to understand the isotopic fractionations that are occurring naturally.

The second part of the presented thesis is dealing with the characterisation of the well core from BH 10-2008 that has been drilled in the Central Tertiary basin of Svalbard, containing Paleocene to Eocene sediments. The focus was to understand the depositional system of those sedimentary sequences as well as to gain insights into the molecular fractionation of generated and expelled hydrocarbons in the respective area.

The depositional setting described in the second paper demonstrated the transition from a subaquatic dominated depositional system towards shallow marine and deltaic deposition in the upper Eocene formations. A key finding is the high impact

of microbial sulphate reduction on the organic matter deposited during the Paleocene Eocene transition, resulting in reduced TOC concentrations and a poor preservation state of the organic matter. Interestingly, other parameters pointed towards favourable organic carbon preserving conditions during the Paleocene Eocene transition.

The impact of microbial sulphate reduction on the reactive proportion of the organic matter could be further supported in paper III. The bulk isotopic composition of the TOC of the respective Paleocene Eocene transition sample exhibits a lighter carbon isotopic composition than the isotopic composition of the reactive organic matter. In combination with a reduced isotopic fractionation of the S2 proportion of the organic matter, we confirmed that the overall preservation state of the organic matter contained in the Paleocene Eocene transition sediments is poor.

Nevertheless, a sediment layer containing elevated organic carbon concentrations (2.7 % TOC) was found to be located directly below the Paleocene to Eocene transition. In order to gain further insights into the thermal maturity of the investigated well section, and to get a better understanding of the molecular maturity proxies that are commonly used to determine the thermal maturity of rock extracts and bitumen, the study described in manuscript IV was conducted. By application of multivariate statistics, a set of seven maturity proxies was selected that showed the best correlation with depth. It was demonstrated that the kerogen maturity is to some extent decoupled from extract maturity. Especially in the Paleocene Eocene transition and adjacent sequences it was evident that many of the parameters deviated from a straight maturity trend.

Since an elevated hydrogen index and a reduction in the Tmax readings was observed for the sediments of the lower Frysjaodden Fm., this area was subjected to further investigations, which are described in paper V.

Elevated hydrogen indices and a reduction in the Rock-Eval Tmax is frequently associated with bitumen staining or hydrocarbon migration. Therefore, the sedimentary sequences above and beneath the Paleocene Eocene transition were selected for a more detailed study regarding hydrocarbon generation, expulsion and the associated

molecular fractionation. The sediments beneath the negative carbon isotopic excursion (below the PETM) contained significant amounts of asphaltenes and polar compounds that are retained in the organic rich layer. The saturated fraction proportion of the generated hydrocarbon migrated upwards into a low organic carbon containing section. The expulsion of bitumen has likely contributed to (i) the molecular fractionation of the measured compounds and compound classes and (ii) has contributed to the elevated values of the hydrogen index and the reduced Tmax values. By applying a modified back-calculation approach and using extract yields and $S2_{ex}$ instead of the standard Rock-Eval parameters, it was possible to calculate realistic volumes of hydrocarbons that have been generated, expelled and migrated.

5.2 Oulook

The presented PhD has used well BH 10-2008 as case study to introduce new concepts and analytical instrumentation. Those concepts need to be applied to other locations or need to be expanded within the Central Tertiary Basin of Svalbard.

For the findings presented in paper III (Rock-Eval isotopic measurements), it would be beneficial to use samples from a natural maturity series and investigate them with the new analytical system. Those results might help to get a better understanding of the natural isotopic fractionating occurring in the reactive organic matter proportion. A source rock to oil correlation in a setting where the source rock has already been linked to a specific oil accumulation might be used to compare the isotopic composition of the S1 and S2 in the source rock with the reservoir fluids. The results could help to understand the secondary migration induced isotopic fractionation better.

The results presented in paper IV provide insights into the qualitative response of maturity markers in rock extracts. In order to advance on the molecular processes occurring in the subsurface affecting those maturity parameters, a quantitative model is needed which uses quantified molecular data for specific compounds. Solubility, polarity parameters, and mass balance calculations might help to gain further insights into the molecular processes during hydrocarbon generation and expulsion. The

necessary data for this approach has been generated during the PhD thesis and should be used to establish a more realistic molecular scale subsurface model. In addition, the study area should be extended to other locations/regions and to source rock sequences of economic value. This might also provide the opportunity to test the unitless maturity indicator on petroleum samples and the corresponding source rocks.

The back-calculation approach presented in paper V used a TR_{mix} that was based on the elemental concentration of carbon and nitrogen. The proposed method might be refined with a more direct measurement of the kerogen type, for example maceral analyses. The main advantage of this modification would be that effects introduced by thermal maturation and initial diagenetic processes on the nitrogen content of the sample material can be avoided.

The investigated area of the CTB is partially covered with 2 D seismic. In a further study the proposed concepts and back-calculation approached should be applied in a numeric simulation model and compare the results with a conventional basin model. Although the amounts of generated and expelled hydrocarbon were quantified, a migration loss, for example through the internal, lateral migration of hydrocarbon in the source interval itself, could not be calculated or estimated.

References

Allen, P. A., and Allen, J. R., (2013): Basin Analyses: Principles and Application to Petroleum Play Assessment (Third Edition). Published by John Wiley & Sons, Ltd.

Banerjee, A., Sinha, A., Jain, A., Thomas, N., Misra, K., Chandra, K., 1998. A mathematical representation of Rock Eval hydrogen index vs Tmax profiles. Organic geochemistry 28, 43-55.

Behar, F., Beaumont, V., Penteado, H.D.B., 2001. Rock-Eval 6 technology: performances and developments. Oil & Gas Science and Technology 56, 111-134.

Bruhn, R., Steel, R., 2003. High-resolution sequence stratigraphy of a clastic foredeep succession (Paleocene, Spitsbergen): An example of peripheral-bulge-controlled depositional architecture. Journal of Sedimentary Research, 73(5), 745-755.

Cui, Y., Kump, L. R., Ridgwell, A. J., Charles, A. J., Junium, C. K., Diefendorf, A. F., and Harding, I. C., 2011. Slow release of fossil carbon during the Palaeocene–Eocene Thermal Maximum. Nature Geoscience, 4(7), 481.

Dallmann, W. K., 1999. Lithostratigraphic lexicon of Svalbard. Norwegian Polar Institute.

Dypvik, H., Riber, L., Burca, F., Rüther, D., Jargvoll, D., Nagy, J., and Jochmann, M., 2011. The Paleocene–Eocene thermal maximum (PETM) in Svalbard—clay mineral and geochemical signals. Palaeogeography, Palaeoclimatology, Palaeoecology, 302(3-4), 156-169.

Elvebakk, H., Rønning, J.S., Jochman, M., Henningsen, T., Johannessen, E.P., Bering, D. and Elvebakk, G., 2008. Geophysical borehole logging in Dh 10-2008 at Sysselmannbreen, Svalbard. NGU Rep., 2008.090, 1–34.

England, W., Mackenzie, A., Mann, D., Quigley, T., 1987. The movement and entrapment of petroleum fluids in the subsurface. Journal of the Geological Society 144, 327-347

Ertas, D., Kelemen, S.R., Halsey, T.C., 2006. Petroleum expulsion part 1. Theory of kerogen swelling in multicomponent solvents. Energy & Fuels 20, 295-300.

Eseme, E., Littke, R., Krooss, B., Schwarzbauer, J., 2007. Experimental investigation of the compositional variation of petroleum during primary migration. Organic Geochemistry 38, 1373-1397

Gavrilov, Y., Shcherbinina, E., Golovanova, O., and Pokrovsky, B., 2009. A variety of PETM records in different settings, northeastern Peri-Tethys. In Climatic and Biotic Events of the Paleogene [CBEP 2009], Extended Abstracts from an International Conference in Wellington, New Zealand, GNS Science Miscellaneous Series, Vol. 18, pp. 67-70.

Grundvåg, S. A., Johannessen, E. P., Helland-Hansen, W., and Plink-Björklund, P., 2014. Depositional architecture and evolution of progradationally stacked lobe complexes in the Eocene Central Basin of Spitsbergen. Sedimentology, 61(2), 535-569.

Han, Y., Horsfield, B., Wirth, R., Mahlstedt, N., Bernard, S., 2017. Oil retention and porosity evolution in organic-rich shales. AAPG Bulletin 101, 807-827.

Han, Y., Mahlstedt, N., Horsfield, B., 2015. The Barnett Shale: Compositional fractionation associated with intraformational petroleum migration, retention, and expulsion. AAPG Bulletin 99, 2173-2202.

Harding, I. C., Charles, A. J., Marshall, J. E., Pälike, H., Roberts, A. P., Wilson, P. A., and Pearce, R. B., 2011. Sea-level and salinity fluctuations during the Paleocene–Eocene thermal maximum in Arctic Spitsbergen. Earth and Planetary Science Letters, 303(1-2), 97-107.

Helland Hansen, W., 1992. Geometry and facies of Tertiary clinothems, Spitsbergen. Sedimentology, 39(6), 1013-1029.

Horsfield, B., and Rullkotter, J., 1994. Diagenesis, Catagenesis, and Metagenesis of Organic Matter: Chapter 10: Part III. Processes 189-199.

Johannessen, E.P., Henningsen, T., Bakke, N.E., Johansen, T.A., Ruud, B.O. and Riste, P., 2011. Paleogene clinoform succession on Svalbard expressed in outcrops, seismic logs and cores. First Break, 29, 35–44.

Kelemen, S., Walters, C., Ertas, D., Kwiatek, L., Curry, D., 2006. Petroleum expulsion part 2. Organic matter type and maturity effects on kerogen swelling by solvents and thermodynamic parameters for kerogen from regular solution theory. Energy & fuels 20, 301-308.

Killops, S. D., and Killops, V. J., 2005. An introduction to organic geochemistry – 2nd ed. 393 p., Blackwell Publishing.

Lallier-Verges, E., Bertrand, P., & Desprairies, A., 1993. Organic matter composition and sulfate reduction intensity in Oman Margin sediments. Marine Geology, 112(1-4), 57-69.

Leythaeuser, D., Littke, R., Radke, M., Schaefer, R., 1988a. Geochemical effects of petroleum migration and expulsion from Toarcian source rocks in the Hils syncline area, NW-Germany, Organic Geochemistry in Petroleum Exploration. Elsevier, pp. 489-502.

Leythaeuser, D., Mackenzie, A., Schaefer, R.G., Bjoroy, M., 1984. A novel approach for recognition and quantification of hydrocarbon migration effects in shale-sandstone sequences. AAPG Bulletin 68, 196-219.

Leythaeuser, D., Radke, M., Willsch, H., 1988b. Geochemical effects of primary migration of petroleum in Kimmeridge source rocks from Brae field area, North Sea. II: Molecular composition of alkylated naphthalenes, phenanthrenes, benzo-and dibenzothiophenes. Geochimica et Cosmochimica Acta 52, 2879-2891.

Leythaeuser, D., Schaefer, R., 1984. Effects of hydrocarbon expulsion from shale source rocks of high maturity in Upper Carboniferous strata of the Ruhr area, Federal Republic of Germany. Organic geochemistry 6, 671-681.

Leythaeuser, D., Schaefer, R., Pooch, H., 1983. Diffusion of light hydrocarbons in subsurface sedimentary rocks. AAPG Bulletin 67, 889-895.

Leythaeuser, D., Schaefer, R., Radke, M., 1988c. Geochemical effects of primary migration of petroleum in Kimmeridge source rocks from Brae field area, North Sea. I: Gross composition of C15+-soluble organic matter and molecular composition of C15+-saturated hydrocarbons. Geochimica et Cosmochimica Acta 52, 701-713.

Livsic, J., 1974. Palaeogene deposits and the platform structure of Svalbard.

Lückge, A., Ercegovac, M., Strauss, H., and Littke, R., 1999. Early diagenetic alteration of organic matter by sulfate reduction in Quaternary sediments from the northeastern Arabian Sea. Marine Geology, 158(1-4), 1-13.

Lüthje, C. J., 2008. Transgressive development of coal-bearing coastal plain to shallow marine setting in a flexural compressional basin, Paleocene, Svalbard, Arctic Norway.

Mackenzie, A., Leythaeuser, D., Schaefer, R., Bjorøy, M., 1983. Expulsion of petroleum hydrocarbons from shale source rocks. Nature 301, 506.

Mann, U., Hantschel, T., Schaefer, R., Krooss, B., Leythaeuser, D., Littke, R., Sachsenhofer, R., 1997. Petroleum migration: mechanisms, pathways, efficiencies and numerical simulations, Petroleum and basin evolution. Springer, pp. 403-520.

Manum, S.B. and Throndsen, T., 1986. Age of Tertiary formations on Spitsbergen. Polar Res., 4, 103–131.

Marshall, C., Large, D. J., Meredith, W., Snape, C. E., Uguna, C., Spiro, B. F.,and Friis, B., 2015a. Geochemistry and petrology of Palaeocene coals from Spitsbergen—Part 1: Oil potential and depositional environment. International Journal of Coal Geology, 143, 22-33.

Marshall, C., Uguna, J., Large, D. J., Meredith, W., Jochmann, M., Friis, B., and Orheim, A., 2015b. Geochemistry and petrology of palaeocene coals from Spitzbergen—Part 2: Maturity variations and implications for local and regional burial models. International Journal of Coal Geology, 143, 1-10.

Mortimer, C. E., and Müller U., 2007. Das Basiswissen der Chemie. 9. Auflage, Georg Thieme Verlag 2007.

Müller, R. D., and Spielhagen, R. F., 1990. Evolution of the Central Tertiary Basin of Spitsbergen: towards a synthesis of sediment and plate tectonic history. Palaeogeography, Palaeoclimatology, Palaeoecology, 80(2), 153-172.

Nagy, J., 2005. Delta-influenced foraminiferal facies and sequence stratigraphy of Paleocene deposits in Spitsbergen. Palaeogeography, Palaeoclimatology, Palaeoecology 222, 161–179.

Nagy, J., Jargvoll, D., Dypvik, H., Jochmann, M., & Riber, L., 2013. Environmental changes during the Paleocene–Eocene Thermal Maximum in Spitsbergen as reflected by benthic foraminifera. Polar Research, 32(1), 19737.

Nøttvedt, A., Livbjerg, F., and Midbøe, P. S., 1988. Tertiary deformation of Svalbard—various models and recent advances. Tertiary Tectonics of Svalbard. Norsk Polarinstitutt Rapportserie, 46, 79-84.

Øygard, Ø. B., 2016. A study of the ichnology, lithology and reservoir quality of the Palaeogene Grumantbyen Formation on Svalbard (Master's thesis, The University of Bergen).

Peters, K.E., Walters, C.C., Moldowan, J.M., 2005. The Biomarker Guide. Biomarkers and Isotopes in Petroleum Systems and Earth History, vols. 1 and 2, Cambridge University Press, USA, p. 1155.

Petersen, T. G., Thomsen, T. B., Olaussen, S., and Stemmerik, L., 2016. Provenance shifts in an evolving Eurekan foreland basin: The Tertiary Central Basin, Spitsbergen. Journal of the Geological Society, 173(4), 634-648.

Pohl, L. W., and Petrascheck, W. E., 2005. Mineralische und Energie-Rohstoffe. Eine Einführung zur Entstehung und nachhaltigen Nutzung von Lagerstätten. 2005 by E. Schweizerbart'sche Verlagsbuchhandlung (Nägele u. Obermiller), Stuttgart.

Radke, M., Willsch, H., and Welte, D. H., 1980. Preparative hydrocarbon group type determination by automated medium pressure liquid chromatography. Analytical Chemistry, 52, 406–411.

Ritter, U., 2003. Solubility of petroleum compounds in kerogen: implications for petroleum expulsion. Organic Geochemistry 34, 319-326.

Ritzmann, O., Jokat, W., Mjelde, R., and Shimamura, H., 2002. Crustal structure between the Knipovich Ridge and the Van Mijenfjorden (Svalbard). Marine Geophysical Researches, 23(5-6), 379-401.

Romero-Sarmiento, M.-F., Pillot, D., Letort, G., Lamoureux-Var, V., Beaumont, V., Huc, A.-Y., Garcia, B., 2016. New Rock Eval method for characterization of unconventional shale resource systems. Oil & Gas Science and Technology–Revue d'IFP Energies nouvelles 71, 37.

Sluijs, A., Schouten, S., Pagani, M., Woltering, M., Brinkhuis, H., Damsté, J. S. S., and Matthiessen, J., 2006. Subtropical Arctic Ocean temperatures during the Palaeocene/Eocene thermal maximum. Nature, 441(7093), 610.

Soliman, M. F., Aubry, M. P., Schmitz, B., and Sherrell, R. M., 2011. Enhanced coastal paleoproductivity and nutrient supply in Upper Egypt during the Paleocene/Eocene Thermal Maximum (PETM): Mineralogical and geochemical evidence. Palaeogeography, Palaeoclimatology, Palaeoecology, 310(3-4), 365-377.

Stainforth, J., Reinders, J., 1990. Primary migration of hydrocarbons by diffusion through organic matter networks, and its effect on oil and gas generation. Organic Geochemistry 16, 61-74.

Steel, R.J., Dalland, A., Kalgraff, K. and Larsen, V., 1981. The Central Tertiary Basin of Spitsbergen: sedimentary development of a Sheared-Margin Basin. In: Geology of the North Atlantic Borderland (Eds J.W. Kerr and A.J. Ferguson), Can. Soc. Petrol. Geol. Mem., 7, 647–664.

Steel, R.J., Gjelberg, J., Helland-Hansen, W., Kleinspehn, K., Nøttvedt, A. and Rye-Larsen, M., 1985. The Tertiary strike-slip basins and orogenic belt of Spitsbergen. SEPM Spec. Publ., 37, 339–359.

Stein, R., Boucsein, B., and Meyer, H., 2006. Anoxia and high primary production in the Paleogene central Arctic Ocean: First detailed records from Lomonosov Ridge. Geophysical Research Letters, 33(18).

Stockhausen, M., Galimberti, R., Di Paolo, L., Elias, R., Gelin, F., Berner, U., Erdmann, M., Pedersen, J.H., Di Primio, R., Schwark, L., 2019. The Expulsinator device: A new approach for a lab-scaled, near-natural generation-and expulsion simulation. Journal of Petroleum Science and Engineering 177, 69-78.

Thomas, M.M., Clouse, J.A., 1990a. Primary migration by diffusion through kerogen: I. Model experiments with organic-coated rocks. Geochimica et Cosmochimica Acta 54, 2775-2779.

Thomas, M.M., Clouse, J.A., 1990b. Primary migration by diffusion through kerogen: II. Hydrocarbon diffusivities in kerogen. Geochimica et Cosmochimica Acta 54, 2781-2792.

Thomas, M.M., Clouse, J.A., 1990c. Primary migration by diffusion through kerogen: III. Calculation of geologic fluxes. Geochimica et Cosmochimica Acta 54, 2793-2797.

Tissot, B.P., Welte, D.H., 1984. Petroleum Formation and Occurrence, Second Revised and Enlarged Edition. Springer, Berlin.

Vandenbroucke, M., Bordenave, M.L., Durand, B., 1993. Transformation of Organic Matter with Increasing Burial of Sediments and the Formation of Petroleum in Source Rocks. In: Bordenave, M.L. (Ed.), Applied Petroleum Geochemistry. Éditions Technip, Paris, pp. 101-122.

Vető, I., Hetényi, M., Demény, A., and Hertelendi, E., 1994. Hydrogen index as reflecting intensity of sulphidic diagenesis in non-bioturbated, shaly sediments. Organic Geochemistry, 22(2), 299-310.

Weiss, H.M., Wilhelms, A., Mills, N., Scotchmer, J., Hall, P.B., Lind, K. and Brekke, T., 2000. NIGOGA - The Norwegian Industry Guide to Organic Geochemical Analyses [online]. Edition 4.0 Published by Norsk Hydro, Statoil, Geolab Nor, SINTEF Petroleum Research and the Norwegian Petroleum Directorate. 102 pp [14.11.2019]. Available from World Wide Web: http://www.npd.no/engelsk/nigoga/default.htm

Ziegs, V., Horsfield, B., Skeie, J.E., Rinna, J., 2017. Petroleum retention in the Mandal Formation, Central Graben, Norway. Marine and Petroleum Geology 83, 195-214.

Paper III

Carbon isotopic analysis of reactive organic matter using a new pyrolysis-cryotrapping-isotope ratio mass spectrometry method: The isotope variation of organic matter within the S1 and S2 peaks of Rock-Eval

Organic Geochemistry 136 (2019) 103886

Contents lists available at ScienceDirect

Organic Geochemistry

journal homepage: www.elsevier.com/locate/orggeochem

Carbon isotopic analysis of reactive organic matter using a new pyrolysis-cryotrapping-isotope ratio mass spectrometry method: The isotope variation of organic matter within the S1 and S2 peaks of Rock-Eval

M. Dörner [a,*], U. Berner [b], M. Erdmann [b], T. Barth [a]

[a] University of Bergen, Chemistry Institute, Allégt. 41, 5007 Bergen, Norway
[b] Equinor AS, Sandslivegen 90, 5254 Sandsli, Norway

ARTICLE INFO

Article history:
Received 4 February 2019
Received in revised form 16 June 2019
Accepted 21 June 2019
Available online 25 June 2019

Keywords:
Organic matter characterization
Isotopic fractionation
Organic matter preservation
Organic matter maturation

ABSTRACT

The source material, the mode of photosynthesis, the organic matter (OM) type, the paleoenvironmental conditions and thermal degradation all determine the isotopic composition of OM. This study presents a novel analytical technique and demonstrates its potential to enhance the understanding of the preservation and maturation-related isotopic compositional changes in OM from different paleoenvironments. A new Rock-Eval type pyrolysis coupled to isotope ratio mass spectrometry (py-IRMS) method has been developed to monitor the isotopic changes during Rock-Eval type pyrolysis while simultaneously recording pyrograms to obtain S1 and S2 peaks compatible with standard Rock-Eval pyrolysis. An automated cryotrapping method allows the sequential sampling of product from defined pyrolysis portions. Each subsample is subsequently transferred to the isotopic ratio mass spectrometer for carbon isotopic measurements. In addition, the cryotrap serves to focus sample peaks, enabling robust and reproducible results even at standard Rock-Eval heating rates. In combination with a standard elemental analyser coupled to an isotopic ratio mass spectrometer (EA–IRMS) it was possible to deconvolute the carbon isotope composition of the reactive components, bitumen and inert components of OM. This allowed us to observe depositional control as well as changes imposed by maturation. Our initial results show the potential of the proposed isotopic screening method to deduce a variety of organic geochemical properties of different OM types based on differences in their carbon isotope compositions. Our results suggest that the ability to produce significant isotopic fractionation during the proposed pyrolysis method is highly dependent on the preservation state of the OM and the thermal maturity.

1. Introduction

From the perspective of pyrolysis, organic matter in sedimentary rocks (i.e. kerogen and coal) has conveniently been considered to consist primarily of two fractions (Fig. 1); the reactive fraction (also called labile plus refractory or pyrolyzable fraction) and the inert fraction (Cooles et al., 1986; Pepper and Corvi, 1995). The reactive kerogen is especially relevant for oil and gas generation with increasing thermal maturation, whilst the inert part is the more abundant fraction in most samples (cf. Jarvie et al., 2005). The latter does not contribute to oil and gas production. To quantify the reactive and inert proportion of the OM in geological sediment samples, pyrolysis techniques have been utilized for decades. Rock-Eval type open pyrolysis (Espitalié et al., 1977, 1985a, 1985b, 1986) allows for rapid evaluation of the amount, thermal maturity, and bulk composition of OM in sediment samples. Based on the remaining hydrocarbon potential (HI) and the oxygen index (OI), an approximation of the organic matter type is possible. A classic differentiation into types of organic matter (kerogen types I, II and III, and sulfur-rich equivalents II-S and I-S) was suggested by Tissot and Welte (1978).

Stable isotope techniques have been established to characterize organic matter in general and to allow for kerogen typing. This has been one of the basic approaches to link reservoir petroleum to its precursors, and consequently, isotope methods have been extended to the characterization of petroleum liquids and their fractions (saturate hydrocarbons, aromatic hydrocarbons, hetero-compound-containing fractions i.e. resins and asphaltenes) to evaluate their possible organic sources (Stahl and Carey, 1975;

* Corresponding author.
E-mail address: markus.doerner@uib.no (M. Dörner).

https://doi.org/10.1016/j.orggeochem.2019.06.007
0146-6380/

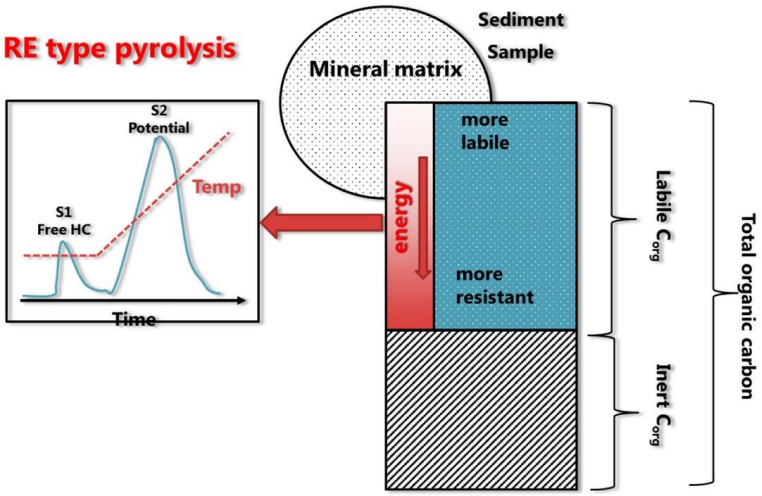

Fig. 1. Schematic overview of the prominent constituents of organic matter. The left corner contains a plot of the pyrolyzable fraction of the organic matter represented as Rock-Eval pyrogram.

Tissot and Welte, 1978; Schoell, 1984; Galimov, 2006) and to differentiate between marine and land plant precursors (Sofer, 1984). In addition, hydrogen isotope ratios of whole oils and oil fractions have been utilized to differentiate between clastic and carbonate-dominated source rocks (Berner, 1982; Waples, 1985).

A concept of organic facies types rather than single kerogen types has been combined with carbon isotope ratios of the bulk organic matter to support the interpretation of the diversity of organic precursors (e.g., Lewan, 1986; Boreham et al., 1994; Stockar et al., 2013). Organic facies according to Pepper and Corvi (1995) are strongly related to the hydrocarbon generation potential, which can be described by specific kinetic concepts. Stable isotope ratios, in addition to other parameters such as biomarker inventory and elemental composition, both support a more precise prediction of hydrocarbon generation potential and provide information on the processes of organic matter preservation and accumulation as well as secondary alteration during diagenetic stages (Stahl, 1978; Spiker and Hatcher, 1984; Macko et al., 1993).

Hydrocarbon generation from the reactive portion of organic matter and its subsequent expulsion out of the sediment leads to an isotope fractionation between the original bulk organic matter and the generated hydrocarbon or bitumen fraction, and thus an isotope shift in the residual organic matter (Tocqué et al., 2005; Galimov, 2006).

Different pyrolysis techniques have been described in the literature to elucidate the isotopic fractionation behaviour of the OM, pyrolyzates and extracted OM. Some studies found that, depending on the technique and sample material used, no significant isotopic fractionation could be observed (Peters et al., 1981; Lewan, 1983; Clayton, 1991a) whereas others found fractionation effects of varying extents (e.g., Arneth and Matzigkeit, 1986; Andresen et al., 1993; Hill et al., 2003; Tocqué et al., 2005). In addition, observations of carbon isotopic fractionation in natural systems associated with magmatic intrusions and higher temperatures at higher heating rates have shown similar isotopic fractionation behaviour as produced in the laboratory (Simoneit et al., 1981; Schimmelmann et al., 2009; Brekke et al., 2014).

The magnitude of the isotope fractionation observed in laboratory experiments (isotope shift) depends on the type of organic matter and its preservation stage in terms of microbial processes (Whiticar, 1999; Somsamak et al., 2006). The overall isotope fractionation effect is an imprint of the temperature range where the conversion of organic matter occurs (Cramer et al., 2001; Li et al., 2014). In all organic systems, the intramolecular, and intermolecular thermodynamically ordered isotope distribution factor is found to exert a prime control on the isotope distribution of molecular compounds (Galimov, 1973, 1975). Isotopic fractionation during maturation of reactive OM is also a determining factor for the initial isotopic fractionation between kerogen and hydrocarbon gases (Clayton, 1991b; Berner et al., 1995; Rooney et al., 1995; Berner and Faber, 1996; Lorant et al., 1998). Advanced modelling, like kinetic modelling of oil and gas generation and related isotope fractionation effects, will benefit from access to data from a continuous monitoring of changes in the carbon isotope pool during thermal maturation. This can assist in the understanding of the petroleum systems and hence aid exploration.

An open system pyrolysis approach makes it possible to perform continuous monitoring of pyrolyzates generated through artificial maturation experiments. However, to our knowledge no combined Rock-Eval type IRMS coupling methodology for a quick and reliable OM characterization is available. Therefore, we describe here a combination of open pyrolysis and isotope classification methods that provides a new technology which allows for a rapid classification of OM in sediment samples. This method enables the user to determine carbon isotopic ratios for the extractable hydrocarbons (equivalent to the thermal extracted Rock-Eval S1 peak) and the potential reactive fraction (equivalent to the Rock-Eval S2 peak) of the sample during a rapid thermal alteration.

This study describes a method that has the potential to give new insights into carbon isotopic fractionation effects related to thermal maturation, and also to improve our understanding of the depositional environment. In addition, the proposed method can elucidate the characteristic of OM in sediment samples as well as evaluate the isotopic composition of the extractable (S1)

proportion in a rapid and less labour-intensive manner than the classical approaches.

2. Methods and materials

2.1. Sample preparation for pyro-cryotrap-IRMS measurements

All samples were crushed with a mortar and pestle to analytical fine grade. Aliquots of the material were subjected to HCl fumigation for 6 h as described in Komada et al. (2008) in order to remove carbonate from the sample. Pyrolysis quartz glass tubes were preconditioned at 700 °C prior to use in order to remove organic contaminations. Silver capsules used for the elemental analysis were pre-extracted with dichloromethane in a Soxhlet extraction unit to remove impurities and reduce the blank background.

2.2. The open pyrolysis-cryotrap-IRMS method

The py-IRMS analyses were performed on an Agilent 7890B gas chromatograph equipped with a Gerstel cold injection system (CIS 6) with a thermal desorption unit (TDU) and a pyrolyzer unit. Helium was used as carrier gas. The sample chamber was continuously flushed with helium to prevent secondary cracking effects. The temperature program of the pyrolyzer unit was chosen to be identical to the Rock-Eval Bulk method temperature program. A detailed summary of the temperature program for each component is shown in Fig. 2. In contrast to the Rock-Eval method described in Espitalié et al. (1985a, 1985b), the pyrolysis unit and the CIS were kept at room temperature through cooling with two ethanol coolers (Gerstel UPC+) when the sample was lowered into the pyrolyzer unit. The pyrolyzer unit was heated at a rate of 20 °C/s to 300 °C. This allows volatile compounds which are adsorbed to the sample matrix to be analysed. The generated pyrolyzate stream, or effluent, is conducted through a 4 m, 0.250 mm i.d. fused silica transfer line into an Agilent four port capillary flow technology (CFT®) purged splitter unit operated at 5 psi constant pressure. The GC is operated isothermally at a constant 310 °C. The flow into the thermal conductivity detector (TCD), flame ionization detector (FID) and isotopic ratio mass spectrometer (Isoprime 100 and Isoprime GC 5) were controlled by restrictors of different length. Since the GC oven is operated in isothermal mode, the split ratio between the different detector systems stays constant. A cryotrap, consisting of a Dewar flask filled with liquid nitrogen and a coiled fused silica column, was fitted between the combustion oven (Isoprime GC5) and the IRMS (Isoprime 100) detector. Oxidation of the eluting components was performed in a copper oxide filled quartz reactor at 950 °C. A Nafion trap was used to remove water from the combustion gases. A computer-controlled pneumatic piston lowers the coiled column into the Dewar flask (product trap) and subsequently pulls it out for 4 s for product release. Due to the low thermal mass of the fused silica column no additional heating was used. An example of the output of the py-IRMS is shown in Fig. 3. An aliquot of 1–5 mg of the sample powder was introduced into a slotted quartz tube and sealed with quartz wool. The tubes were fitted onto a holder which was automatically lowered sequentially into the pyrolysis unit by a Gerstel multipurpose sampler equipped with a gripper.

During the first pyrolysis step (related to the standard Rock-Eval S1, at 300 °C), CO_2 eluting from the combustion oven is trapped. After the isothermal phase was finished, the trapped sample gas was released and conducted into the isotopic ratio mass spectrometer. During the second phase of pyrolysis (S2) the CO_2 eluting from the combustion oven was stepwise trapped and released for each approximately 15 °C of temperature increase, which made it possible to determine the carbon isotopic composition of different pyrolyzate fractions during the entire pyrolysis process (Fig. 3). Further details on the instrumentation used are described in Doerner et al. (2018).

Since the pyrolysis temperature from our system differed from the Rock-Eval T_{max} reading, we calibrated our measured values according to the procedure described in Behar et al. (2001):

$$\text{Rock-Eval } T_{max} = T_{peak} - 39\,^{\circ}C \quad (1)$$

where T_{peak} is the measured pyrolysis temperature at the maximum response of the S2 peak. In the cases where the calculated corresponding Rock-Eval T_{max} lies in between two sampling points of the cryotrap, the T_{max} isotopic composition is approximated and averaged within those two sampling temperature intervals.

The stable isotope composition of carbon is reported in delta (δ) units as the per mil deviation (‰) of the isotopic ratio relative to a known standard:

$$\delta = \left[\frac{R_{Sample} - R_{Standard}}{R_{Standard}}\right] \times 1000 \quad (2)$$

where R is the ratio of $^{13}C/^{12}C$. All measurements were normalized to Vienna Pee Dee Belemnite (VPDB).

CO_2 monitor gas of known isotopic composition was used as a single point anchor for the isotopic measurements. Two pulses of the monitor gas were inserted prior to and following the eluted sample peaks. The normalization of the py-IRMS measured $\delta^{13}C$ values to the VPDB scale was performed by pyrolysis of a sulphanilamide standard of known carbon isotope composition. The $\delta^{13}C$ value (−27.8‰ ± 0.03‰) of this in-house pyrolysis standard was previously determined by EA–IRMS (see Section 2.3). To assess the extent of possible isotopic fractionations, the sulphanilamide was subjected to Rock-Eval pyrolysis five times in order to evaluate the pyrolyzable organic carbon (PC) and the residual organic carbon (RC) cf. Behar et al. (2001). The results were approximately

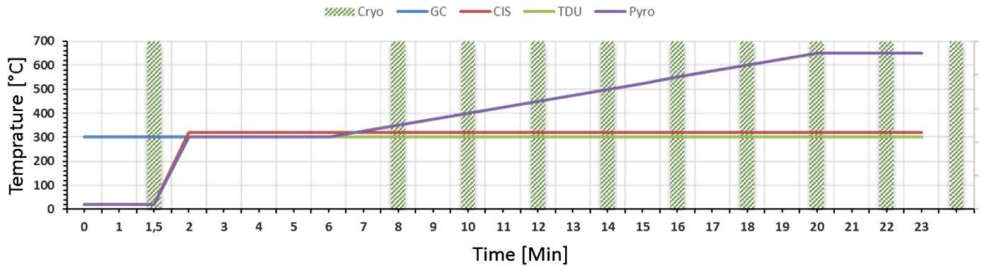

Fig. 2. Overview over the temperature of each component of the utilized system against time. Green bars mark the sampling of the automated cryotrapping device in this case set to an interval of 2 min. (For interpretation of the references to colour in this figure legend, the reader is referred to the web version of this article.)

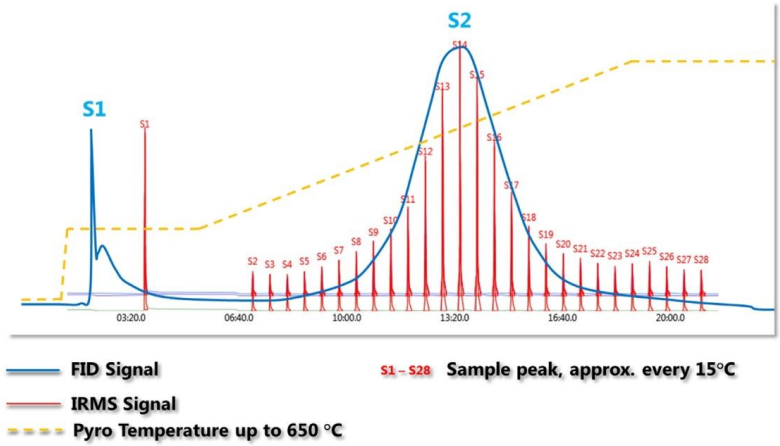

Fig. 3. Overview of the chromatographic results from the py-IRMS system. FID and IRMS signal are recorded simultaneously. The blue line represents the Rock-Eval type pyrogram including the S1 and S2 peaks. The red peaks and labels represent the chromatographic results detected by the isotopic ratio mass spectrometer. (For interpretation of the references to colour in this figure legend, the reader is referred to the web version of this article.)

1:1 (PC:RC). After pyrolyzing sulphanilamide with the py-IRMS, residual material from the quartz glass tube was subjected to the EA–IRMS. The isotopic values from measurements of the original standard (combined PC and RC) yielded −27.81‰, and −27.76‰ for the residual standard (RC fraction) material after repeated pyrolysis experiments (n = 5). The difference between the two fractions, PC and RC, of ±0.03‰ is within the expected analytical uncertainty. The sulphanilamide standard material was therefore used as calibration standard for the open py-IRMS measurements.

The production of a robust statistic on the repeatability and error of repeated measurements of the instrument is not straightforward because of the timed cryogenic focusing. Small differences in the pyrolysis behaviour of a sample aliquot can lead to changes in the sampled portion performed by the automated cryotrap. For this study, we determined an error of repeated measurements of ±0.3‰ for the S1 fraction and ±0.6‰ for the different S2 fractions.

2.3. Sample characterization with standard Rock-Eval, CNS-elemental and $\delta^{13}C_{org}$ analyses

A Rock-Eval 6 Turbo analyser was used for the identification of kerogen type as well as the measurement of the hydrogen index (HI), thermal maturity, and TOC. Analyses were carried out on at the Equinor AS Research Centre, Sandsli Norway, by selecting the Rock-Eval basic method (sometimes referred to as the bulk method) as describes in Behar et al. (2001). All measurements were run in triplicate and calibrated with IFP16000, JR-1 and SR-1 standard materials.

Elemental and bulk isotopic analyses were performed on an Elementar Pyro Cube coupled to an Isoprime 100 isotope ratio mass spectrometer. The pyro cube was operated in CNS mode to obtain total carbon (TC), total nitrogen (TN) and total sulfur (TS) values for the untreated crushed samples. The combustion temperature was set to 1120 °C and the reduction temperature was set to 850 °C. The oxygen flush time was adjusted to 15 s. $\delta^{13}C_{TOC}$ values were obtained by analysing the HCl fumigated sample material with the same system settings. Silver capsules were used as packing material. Normalization of the elemental analysis was accomplished by calibration against a sulphanilamide standard. Normalization of the IRMS measurements was done by use of the coffeine 1, 2 and 3 standards (Schimmelmann et al., 2016). Quality control was carried out by analysing JR-1 and SR-1 standards repeatedly within each sample sequence. Results are expressed in ‰ relative to Vienna Pee Dee Belemnite (V-PDB) standard.

3. Results and discussion

3.1. Bulk organic geochemistry of sample material for the experiments

Ten sediment samples from various locations and different organo-facies representing different kerogen types were obtained from Equinor's sample repository to provide data derived from the new py-IRMS method for use in subsequent interpretations. In order to provide a better traceability of the different samples in this text, sample numbers according to Table 1 are indicated in parenthesis at the relevant position in the text.

Rock-Eval parameters (S1, S2, T_{max}), total organic carbon (TOC), sulfur content (TS), as well as the bulk organic carbon isotopic composition ($\delta^{13}C_{org}$) of a sample, give information on the type of kerogen and on the maturity of the OM present (Espitalié et al., 1977; Schoell, 1984; Leventhal, 1995). A detailed overview of the results for elemental, isotopic and Rock-Eval analyses is given in Table 1.

The highest TOC concentrations were detected within the Aspelintoppen Fm (7) coals and the sandstones containing coal clasts (6). Overall, the TOC for the analysed sample suite varied from 1.1 wt% for the Frysjaodden Fm (8) and Basilika Fm (10) from the Central Basin Svalbard, up to 65.9 wt% for the coal from the Aspelintoppen Fm (7). The sulfur content within the sample suite ranged from 0.9 wt% for the sample from the Messel Fm (2) and Basilika Fm (10), to 6.5 wt% for Whitby Mudstone Fm (4) sample, which is the highest concentration of sulfur within the sample suite.

A characterization of the depositional environment for the samples based on the TS and TOC content is presented in Fig. 4. The samples from the Messel Fm (2), Green River Fm (1), and samples from the Aspelintoppen Fm (6, 7) can be characterized as deposited under lacustrine, pluvial conditions. The samples from the Whitby Mudstone Fm (4), Frysjaodden Fm (8, 9) and the Basilika Fm (10) can be classified as deposited under mixed marine to fully marine

Table 1
Summary of the sample locations, lithology and sample types that have been used for this study and Rock-Eval, total sulfur and $\delta^{13}C_{TOC}$ measurements. Please note that sample 1–5 are outcrop samples whereas samples 6–10 are core samples.

Sample no	Formation	Location/Well	Lithology	T_{max} [°C]	HI [mg/g TOC]	TOC [wt%]	Sulfur [wt%]	$\delta^{13}C_{TOC}$ [‰ VPDB]
1	Green River Fm. Mahogany Shale	Sweetwater River	Shale	436	488	21.1	2.4	−29.35
2	Messel Fm.	Messel Pit	Shale	425	601	22.6	0.9	−29.32
3	Svalbard Rock (Botneheia Fm.)	Svalbard	Shale	439	259	2.3	1.3	−31.53
4	Jet Rock (Whitby Mudstone Fm.)	Kimmeridge Bay UK	Shale	431	609	12.3	6.5	−32.39
5	Wealden Fm.	Dorset UK	Clay/Sand	416	425	6.51	3.1	−28.08
6	Aspelintoppen Fm.	Svalbard BH 10-2008	Sand Coalclasts	422	261	24.8	3.1	−25.11
7	Aspelintoppen Fm.	Svalbard BH 10-2008	Coal	422	360	65.9	3.8	−28.33
8	Frysjaodden Fm.	Svalbard BH 10-2008	Shale	445	180	1.1	2.2	−30.27
9	Frysjaodden Fm.	Svalbard BH 10-2008	Shale	447	136	2.4	1	−26.78
10	Basilika Fm.	Svalbard BH 10-2008	Shale	448	117	1.1	0.9	−26.82

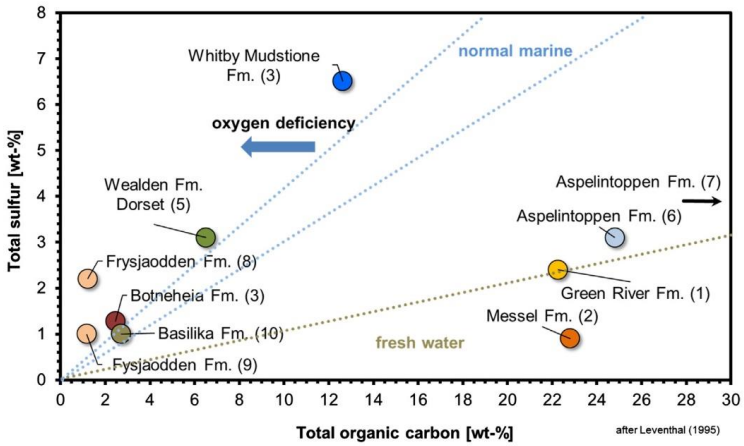

Fig. 4. Plot of total organic carbon vs total sulfur (modified after Leventhal, 1995). The sample material used for this study covers a wide range of different depositional environments.

conditions with varying availability of oxygen (i.e. reducing conditions).

Fig. 5 shows the remaining hydrocarbon generation potential (HI) and the present-day thermal maturity of the investigated samples. We include kerogen type curves based on information given in Bordenave (1993) and Banerjee et al. (1998) as reference information for an initial evaluation of our sample set. Rock-Eval measurements reveal a T_{max} variation from 416 °C up to 448 °C T_{max} within the sample suite. The highest HI values are present for the Whitby Mudstone Fm (4) sample (HI of 609 mg/g TOC) and the Messel Fm (2) shale sample (HI of 601 mg/g TOC). The lowest HI values of 117–180 mg/g TOC, and highest T_{max} values are represented by the samples from well BH 10–2008 Svalbard (8–10).

Except for the samples from the Frysjaodden Fm (8, 9) and the Basilika Fm (10), which plot in the intersection of a Type III and a mature Type II kerogen, all the other samples are classified as kerogen Type II. Those findings only partially agree with the results from the TOC, TS analyses as well as the literature review. The difference is unlikely to be attributed exclusively to maturity effects, since a misrepresentation of the depositional environment is also present for the immature to early mature samples. Most likely the misrepresentation is due to mixing of different kerogen types. Land plant OM input into a Type I kerogen might result in a shift towards Type II (Carrol and Bohacs, 2001) within the HI–T_{max} diagram. In addition, it was reported earlier that variations in the mineral matrix and organic enrichment can affect the hydrogen index of the Rock-Eval. Therefore, those values need to be handled with caution (Katz, 1983).

Published data and interpretations concerning our samples are available from a multitude of sources and will therefore only be briefly reviewed here.

The sample from the Mahogany Oil shale (1), was selected to represent the classical properties of a Type I lacustrine kerogen (Ruble et al., 2001). The Mahogany Oil Shale is part of Eocene Green River Formation which is localized in Utah, Wyoming and Colorado (Surdam and Wolfbauer, 1975; Cole and Picard, 1981; Smoot, 1983). Ruble and Philp (1998) concluded that methanogenic archaea must have been present in a deeper position within the stratified paleo lake, where they contributed to the biodegradation of planktonic algal material while it sank through the water column followed by a subsequent isotopic ^{12}C enrichment of the dissolved lake water which in turn led to an enrichment of the lighter carbon isotope in the planktonic organic matter. More resistant biomass settled into the anoxic offshore lacustrine environment where it was eventually preserved as amorphous kerogen in the Mahogany Oil shales.

One sample from the Eocene Messel shale (2), located near Darmstadt, Germany, which is classified as a Type I kerogen deposited in a lacustrine environment is also included. Matthes (1968) suggests that the Messel sediments were deposited in a series of shallow lakes connected by a slow-moving fluvial system. The Messel Shale was influence by high activity of methanogenic

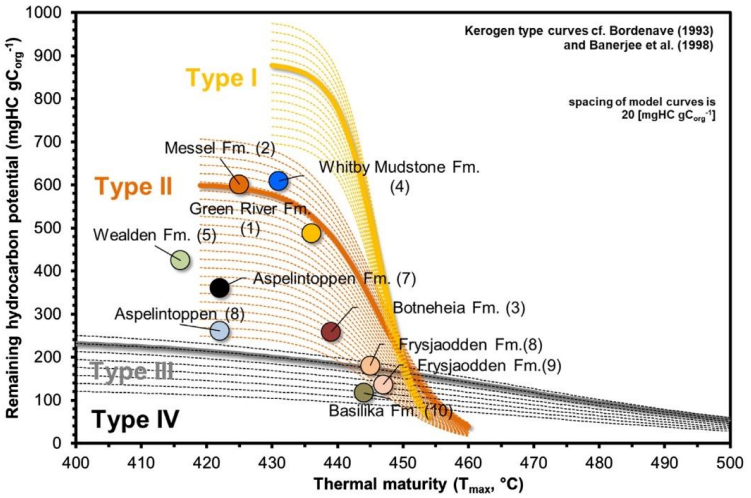

Fig. 5. Plot of thermal maturity expressed in T_{max} vs the remaining hydrocarbon potential (HI). The kerogen type curves as well as the modelled curves are modified after Banerjee et al. (1998) and Bordenave (1993).

archaea. Hayes et al. (1990) found that the $\delta^{13}C$ values of phytane fit with those of archaebacterial lipids in the same section, whereas pristane showed $\delta^{13}C$ values comparable to derivatives of phytol produced by the same organism that produced porphyrins from algal lipids. It was concluded that isotopically light carbon from biogenic methane was incorporated into the sediments (methane recycling), pointing towards highly anoxic conditions in the sediment column and bottom waters (Hayes et al., 1987).

One portion of the Botneheia Fm (3) siliciclastic shale, also known as the Svalbard Rock (SR-1), was included. The material was taken from a section with low organic carbon content in the Anisian, Middle Triassic Botneheia formation. The claystone, which is dominated by mineral matter, was likely deposited under reducing, marginal marine to open marine, conditions. The sample material is part of the Norwegian Geochemical Standards and was collected in 1994 in large amounts for use in organic geochemical laboratories as a reference material (Dahlgren et al., 1998).

The sample from the Whitby Mudstone Fm (4), commonly known as Jet Rock (JR-1) is also part of the Norwegian Geochemical Standard collection. The sample was collected in the vicinity of Port Mulgrave, Yorkshire northeastern England and is according to Howard (1985), Knox (1984) and Powell (1984) a black shale of Upper Jurassic age which was deposited under anoxic conditions (Morris, 1980). The TOC content established within the analytical campaign of standardization is 12.4 wt% (Dahlgren et al., 1998).

The Early Cretaceous Wealden Fm (5) sediments (Allen, 1975, 1981) consist mainly of sandstones and mudstones which were deposited in fluvial to lagoonal conditions. The sample material used for this study was collected in the Mupe Bay area of Dorset, UK. This area is characterized by oil seeps and the sample has an imprint of migrated oil (Wimbledon et al., 1996).

Five samples from the well Svalbard BH 10-2008 were sampled at the core storage of Equinor AS, Sandsli, Norway. They comprise the Basilika Fm (6), Frysjaodden Fm (8, 9), Aspelintoppen Fm (6, 7) within the Tertiary basin of Svalbard. The sample material from this well is especially suitable for this study since no contamination through drilling fluid was detected during the initial geochemical screening. The well section has previously been described by Grundvåg et al. (2014). The Basilika Fm which is located at the deeper part of the well section can be described as a claystone deposited in a pro-delta to offshore setting. The Frysjaodden Fm represents open marine sedimentation and consist of a relatively homogeneous shale, with varying degrees of lamination. Further details have been published by Dypvik et al. (2011). The Aspelintoppen Fm consists mainly of a terrestrially influenced, fluvio-deltaic alternation of clay, silt and sand. This segment also incorporates coal layers of up to 30 cm thickness of which one sandstone with coal clasts and a coal were selected.

The results from the bulk analyses in combination with published data shows that the sample set used for this study represents different organo-facies types (Pepper and Corvi, 1995) with significant differences in their organic geochemical properties. This provides a suitable testing environment for the py-IRMS method.

3.2. Results and discussion of cryotrap-IRMS experiments

Fig. 6 shows a compilation of raw data that has been generated with the py-IRMS method. The samples were pyrolyzed with a Rock-Eval type temperature program. The isotopic value for the thermovaporized compounds in the S1 signal which is eluted at 300 °C is given in Table 2. The sample from the Whitby Mudstone Fm (4) shows that the initial heavy and adsorbed extractable fractions are fully eluted (depending on the rock matrix and composition of the bitumen) at about 350 °C (as described in Romero-Sarmiento et al., 2016) at which point isotopic values become gradually enriched in ^{12}C until the T_{peak} temperature of 495 °C is reached. Initial depletion of the ^{13}C portion during the temperature ramped pyrolysis experiment (until T_{peak} is reached) has been described before. Lorant et al. (1998) as well as Hill et al. (2003) assign this effect to undetermined precursors in the immature kerogen, possibly adsorbed lipids. For the sample set studied here, this kerogen precursor needs to be taken into account since not all samples exhibited higher thermal maturation stages.

At the T_{peak} value, the Whitby Mudstone Fm (4) sample exhibits the lightest isotopic composition of −32.5‰. From the T_{peak} onwards, the isotopic values become depleted in ^{13}C again reaching a value of −29.2‰ at the final temperature stage of 650 °C. The generated isotopic fractionation curve reflects a difference of

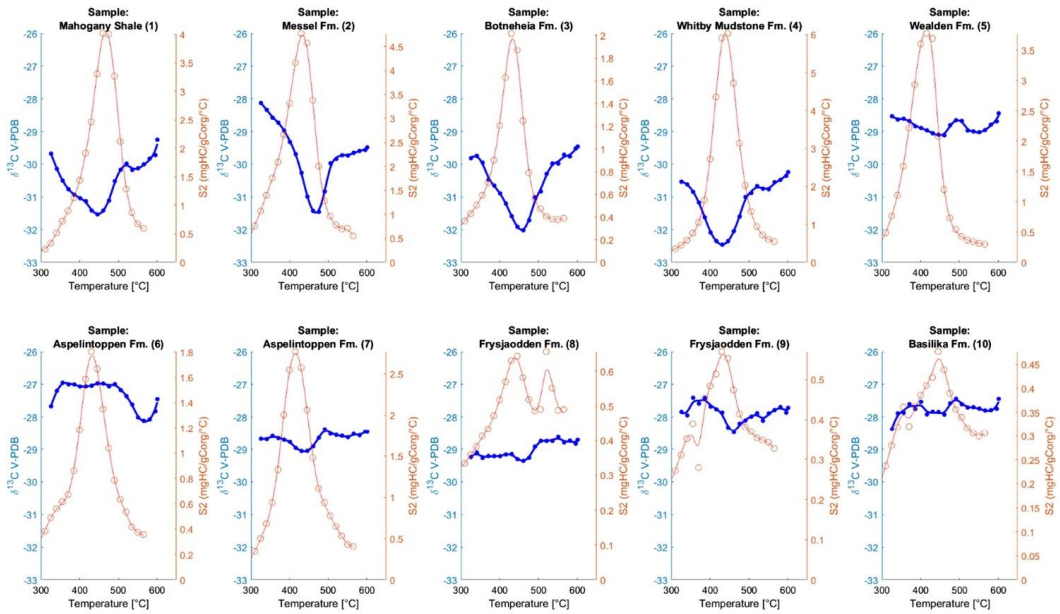

Fig. 6. Data compilation for all samples evaluated with the new py-IRMS methods. The blue dots mark each subsample taken from the cryotrap, as given in Table 2. The red line and dots indicate the S2 evolution from CO_2 detected by the isotope ratio mass spectrometer. Values have been calculated by mass balance. All isotopic data are expressed in $\delta^{13}C$ V-PDB. (For interpretation of the references to colour in this figure legend, the reader is referred to the web version of this article.)

3.2‰ from the heaviest to the lightest isotopic value. This represents the greatest fractionation occurring in the evaluated sample set. In contrast to the Whitby Mudstone Fm (4) sample, all samples from the well Svalbard BH 10-2008 (6–10) show a flat trend of isotopic fractionation with only minor differences between the heaviest and lightest isotopic values.

A full overview on the isotopic measurement reported in relation to the pyrolysis temperature are given in Table 2. The average isotopic composition for the S2 proportion of the different samples varies between −27.8‰ for an organic lean sample from the Basilika Fm (10) to −31.0‰ for the Whitby Mudstone Fm (4) sample. Fig. 7 displays a compilation of isotopic fractionation curves for all analysed samples against the pyrolysis temperature. The isotopic fractionation curves can be separated into three groups. Those three groups can be understood to represent the depositional environments identified by the bulk analyses and the references cited in Section 3.1. The grouping is based on the mass-balanced averaged isotopic value of each group as well as the extent of fractionation. The grey shaded areas represent the span of isotopic variety in the respective groups.

The samples from the Whitby Mudstone Fm (4), Messel Fm (2), Botneheia Fm (3), and Green River Fm (1) (Group 1) are characterized by an extensive isotopic fractionation of up to 3.2‰ and a light average isotopic value. These results can be related to the preservation state of the OM occurring under anoxic condition as described in Lehmann et al. (2002). Therefore, this group is classified as deposited under anoxic conditions with an influence of methane and/or CO_2 recycling. The magnitude of isotopic fractionation seen in the Botneheia Fm (3) sample, is supported by the results from Brekke et al. (2014) who showed that the $\delta^{13}C$ values of extracted OM are heavily affected by elevated temperature close to a sill. The range of isotopic values reported (−32.2‰ to −27.6‰) agrees with our experimental data. As a first approach, we therefore relate the ability to produce significant isotopic fractionation to the preservation state of OM.

The second group (Group 2) consists of a coal sample from the Aspelintoppen Fm (6), the Wealden Fm (5) sample, and the shale sample from the Frysjaodden Fm (9). This group is classified by a unidirectional, almost constant isotopic value around −29.2‰, showing no significant fractionation. This might indicate a homogeneous composition of the OM within those samples, combined with a poor preservation state of the OM, pointing towards dysoxic conditions during the deposition.

The third group (Group 3) incorporates the samples from the Aspelintoppen Fm (5), from the Basilika Fm (10), and from the Frysjaodden Fm (8). Those samples exhibit isotopic average values enriched in ^{13}C and a prominent scatter around their average value. The pluvial shale sample from the Aspelintoppen Fm (5) shows a reverse fractionation trend starting at −27.0‰ and becoming depleted in ^{13}C with increasing pyrolysis temperatures towards the end of the pyrolysis program. We assign this effect to a diverse mixture of different OM types with a significant influence from kerogen Type III.

The artificial maturation process imposed by the pyrolysis technique needs to be considered in order to explain the fractionations curves, especially for highly fractionated samples. As reported by Lewan (1983), the change in the isotopic composition (enrichment of ^{13}C with increasing maturity) might be attributed to an increasing cleavage of the ^{13}C–^{12}C bonds in the generated bitumen during the decomposition process into expelled pyrolyzate. The ^{12}C–^{12}C bonds of the pyrolyzate are preferentially cleaved. The same kinetic isotope effect is reported in Galimov et al. (1972) showing that at 500 °C all the C_1 to C_4 hydrocarbons become isotopically enriched associated with the formation of pyrobitumen. Although extensive heat and a higher heating rate are applied during the analysis, it seems likely that the ability to produce significant

Table 2
Compilation of the isotopic values for the evaluated samples. The highlighted fields mark the corresponding Rock-Eval T_{peak} isotopic values.

	Sample Peaks	Pyrolysis Temperature [°C]	Sample No. 1	2	3	4	5	6	7	8	9	10
S1 and Bitumen	S1	300	–30.5	–29.0	–31.1	–31.0	–28.4	–27.9	–28.9	–29.2	–29.4	–27.8
	S2	330	–30.1	–27.8	–29.8	–30.1	–28.8	–28.3	–29.1	–28.8	–28.4	–28.5
	S3	345	–28.3	–27.8	–29.5	–30.2	–28.8	–28.0	–28.7	–29.0	–28.7	–28.5
	S4	360	–29.0	–28.0	–29.7	–30.3	–28.7	–27.8	–28.7	–29.0	–28.7	–28.6
		S1 Min $\delta^{13}C$	–30.5	–29.0	–31.1	–31.0	–28.8	–28.3	–29.1	–29.1	–29.4	–28.6
		S1 Max $\delta^{13}C$	–28.3	–27.8	–29.5	–30.1	–28.4	–27.8	–28.7	–28.8	–28.4	–27.8
		S1 Average $\delta^{13}C$	–29.5	–28.2	–30.0	–30.4	–28.7	–28.0	–28.9	–29.0	–28.8	–28.3
S2 (HC Potential)	S5	375	–29.7	–28.1	–29.8	–30.5	–28.5	–27.7	–28.7	–29.2	–27.8	–28.4
	S6	390	–30.1	–28.3	–29.7	–30.6	–28.6	–27.2	–28.7	–29.1	–28.0	–27.9
	S7	405	–30.5	–28.6	–30.0	–30.8	–28.6	–27.0	–28.6	–29.3	–27.4	–27.9
	S8	420	–30.8	–28.7	–30.5	–31.2	–28.7	–27.0	–28.7	–29.2	–27.6	–27.6
	S9	435	–30.9	–29.0	–30.7	–31.6	–28.8	–27.0	–28.7	–29.2	–27.4	–27.8
	S10	450	–31.00	–29.3	–30.9	–32.1	–28.9	–27.1	–28.8	–29.2	–27.7	–27.5
	S11	465	–31.1	–29.7	–31.2	–32.4	–29.0	–27.0	–29.0	–29.2	–27.8	–27.9
	S12	480	–31.4	–30.3	–31.6	–32.5	–29.1	–27.0	–29.1	–29.2	–27.9	–27.8
	S13	495	–31.5	–31.0	–31.9	–32.4	–29.1	–27.0	–29.1	–29.3	–28.3	–27.9
	S14	510	–31.4	–31.4	–32.0	–32.1	–29.1	–27.0	–28.9	–29.4	–28.5	–27.9
	S15	525	–31.1	–31.5	–31.7	–31.6	–28.8	–27.0	–28.7	–29.3	–28.2	–27.6
	S16	540	–30.5	–30.8	–31.0	–31.0	–28.7	–27.0	–28.4	–28.9	–28.1	–27.4
	S17	555	–30.1	–30.0	–30.8	–30.9	–28.7	–27.2	–28.5	–28.8	–28.0	–27.6
	S18	570	–30.0	–29.8	–30.3	–30.7	–29.0	–27.4	–28.6	–28.8	–27.9	–27.7
	S19	585	–30.2	–29.7	–30.0	–30.8	–29.0	–27.6	–28.6	–28.8	–28.1	–27.7
	S20	600	–30.1	–29.7	–30.0	–30.8	–29.2	–28.0	–28.6	–28.6	–27.9	–27.7
	S21	615	–30.0	–29.7	–29.7	–30.6	–29.0	–28.1	–28.5	–28.8	–27.8	–27.8
	S22	630	–29.8	–29.6	–29.8	–30.5	–28.8	–28.1	–28.6	–28.7	–27.7	–27.8
	S23	645	–29.7	–29.6	–29.5	–30.4	–28.7	–27.8	–28.5	–28.8	–27.9	–27.8
	S24	650	–29.3	–29.5	–29.5	–30.2	–28.4	–27.5	–28.5	–28.7	–27.7	–27.4
	S25	650	–29.5	–29.6	–29.4	–30.1	–28.3	–27.6	–28.4	–29.0	–27.7	–27.5
	S26	650	–29.2	–29.3	–29.3	–30.2	–28.4	–27.9	–28.1	–29.1	–27.9	–27.7
	S27	650	–29.4	–29.6	–29.5	–29.2	–28.5	–27.8	–28.6	–29.0	–27.6	–27.8
		S2 Min $\delta^{13}C$	–31.5	–31.5	–32.0	–32.5	–29.1	–28.1	–29.1	–29.4	–28.5	–28.4
		S2 Max $\delta^{13}C$	–29.2	–28.1	–29.3	–29.2	–28.3	–27.0	–28.1	–28.6	–27.4	–27.4
		S2 Mass Balance $\delta^{13}C$	–30.8	–30.2	–30.9	–31.6	–28.9	–27.2	–28.8	–29.3	–28.5	–27.8

isotopic fractionation curves is not exclusively dependent on the cleavage of bonds between the stable carbon isotopes. In addition, the OM type of the individual samples and the related OM preservation state, in particular of the reactive part of the OM, seems to have a high impact on the characteristic fractionation performance as the pool of depleted (^{12}C) carbon within the evaluated sample is less affected by previous processes occurring during the deposition of the sample material.

This interpretation is supported by the isotope trend shown in Fig. 8, which shows the isotopic values of the reactive kerogen fraction against the results from the EA–IRMS measurements representing the $\delta^{13}C_{TOC}$ (reactive and inert). The trend in the data cannot be explained through temperature effects on the isotope fractionation, as all samples were subjected to the same procedure, but it must be related to the isotopic signatures of the reactive and inert fraction of the organic matter alone. Indicated by the 1:1 trendline, samples from the Messel Fm (2), Green River Fm (1), Wealden Fm (5), Aspelintoppen Fm (6, 7), Frysjaodden Fm (8), and Basilika Fm (10) exhibit an isotopically depleted composition for the reactive fraction compared to the bulk isotopic composition whereas the remaining samples show the opposite composition.

Furthermore, a comparison between reactive $\delta^{13}C$ and the bulk isotopic composition values helps to separate the three different depositional group types that have previously been identified. The evaluation of $\delta^{13}C_{TOC}$ values exclusively does not separate these three groups. The groups covering anoxic and methane recycling as well as dysoxic to anoxic exhibit a significant overlap in their $\delta^{13}C_{TOC}$ values, making it impossible to separate them further based on the bulk isotopic value. An examination of the isotopic value of the pyrolyzable fraction of OM can therefore add to the understanding of the depositional environment.

To test to what extent the proportion of reactive organic carbon affects the isotopic values of the reactive fraction, and to rule out that our results only represent the amount of reactive organic matter in the different OM types, we calculated the amount of reactive organic carbon according to the following formula:

$$L_{Corg} = \frac{S_2 \times 0.082}{TOC\% - S_1 \times 0.082} \times 100[\%] \quad (3)$$

where L_{Corg} is the labile proportion of the organic matter, S1 is the free hydrocarbon proportion, and S2 is the remaining hydrocarbon potential evaluated from the Rock-Eval measurement. 0.082 is the

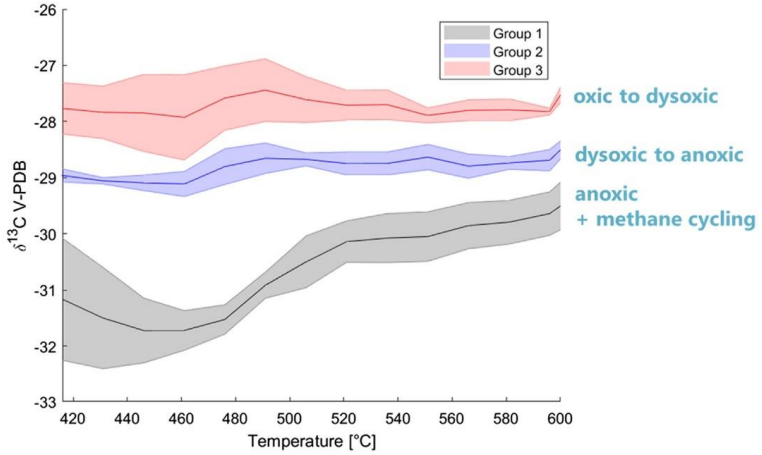

Fig. 7. Pyrolysis temperature vs $\delta^{13}C$ values for the pyrolyzates (S2). The isotopic values are clustered into three separate groups. The solid black, blue and red lines indicate the average of all samples within the respective group. The coloured shaded areas show the range of isotopic compositions present in each group. The groups are labelled with an initial interpretation regarding the depositional environments under which they were deposited. (For interpretation of the references to colour in this figure legend, the reader is referred to the web version of this article.)

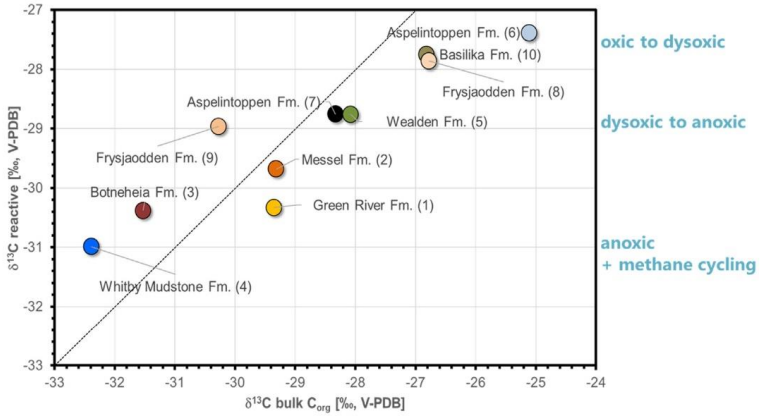

Fig. 8. $\delta^{13}C$ bulk values from EA-IRMS measurements vs averaged $\delta^{13}C$ reactive kerogen values showing the improved separation (highlighted with yellow circles) for the depositional environments. (For interpretation of the references to colour in this figure legend, the reader is referred to the web version of this article.)

assumed proportion of carbon presented in the Rock-Eval S1 and S2 fractions.

Fig. 9 displays a cross plot of the percentage of reactive organic carbon vs the corresponding $\delta^{13}C$ values. A discrimination between immature and oil-mature samples was achieved by utilizing T_{max} values. Some samples fall in the immature field while other samples have maturities within the lower oil window. As expected, sample of higher maturity exhibit overall a lower concentration of reactive organic carbon. However, there is no correlation between the amount of reactive OM and the isotopic composition of the respective sample. The sample from the oil-mature Botneheia Fm (3) with around 20 wt% reactive organic carbon shows an almost identical reactive organic carbon isotopic composition when compared to the Green River Fm (1) and Whitby Mudstone Fm (4) sample which have significantly higher amounts of reactive OM of up to 52 wt%.

Since we observed differences in the isotopic composition for the S1 and S2 proportions, it seems likely that the maturity state of the individual samples might be deducible from the isotopic measurements performed here. Assuming that the pool of oil and or gas generated from the kerogen of a source rock is exclusively restricted to the reactive organic fractions, the difference between the S1 isotopic composition and the T_{peak} (T_{max}) isotopic composition might shed a light on the thermal maturity state. We therefore calculated the $\varepsilon_{Peak\ gen\ -\ S1}$ according to the following formula:

$$\varepsilon_{Peak-gen-S1} = \left|\delta^{13}C_{Tpeak}\right| - \left|\delta^{13}C_{S1}\right| \quad (4)$$

We also tested this assumption for immature and early mature sample materials such as sediment samples from the Wealden Fm (5) (T_{max} of 418 °C) and sample material from the Aspelintoppen Fm (6, 7) (T_{max} of 422 °C). In the early stages of thermal

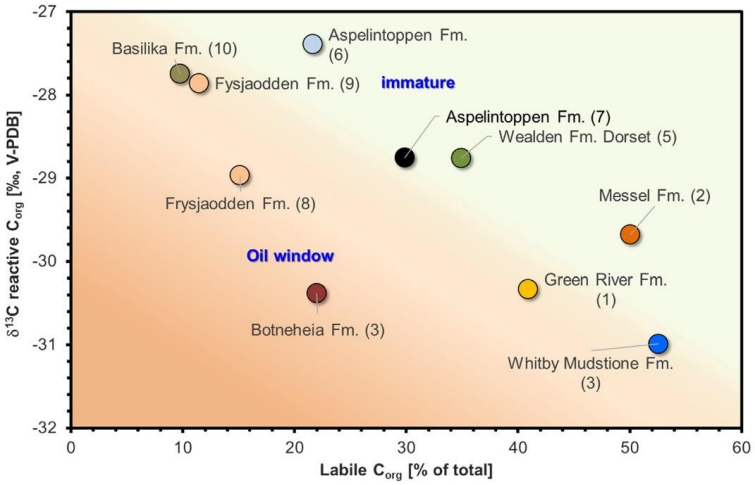

Fig. 9. Proportion of reactive organic carbon vs $\delta^{13}C$ of the reactive fraction, indicating that there is no relationship between the isotopic composition and the amount of reactive organic matter.

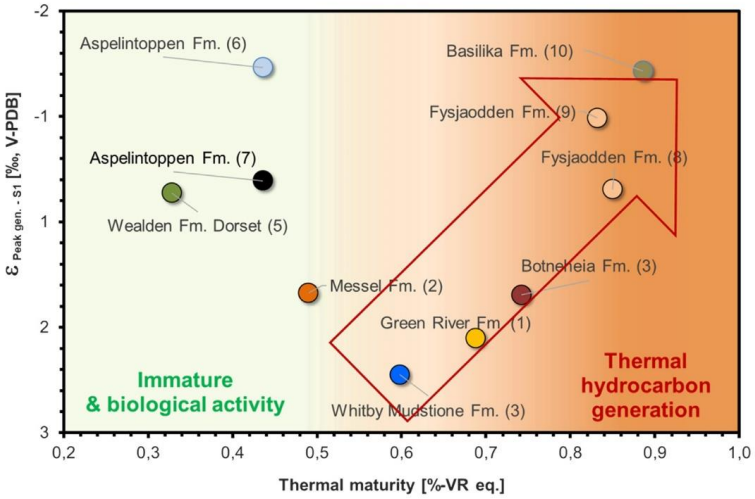

Fig. 10. Maturity indication deduced from $\varepsilon_{Peak\ gen\text{-}S1}$ plotted against Vr_{eq} calculated from Rock-Eval T_{max} values. The red arrow marks the general maturity trend. Samples on the left side are dominated by biological activity and/or diagenesis. Once oil expulsion and primary migration commences, the $\varepsilon_{Peak\ gen\text{-}S1}$ parameter can be used as maturity indicator. (For interpretation of the references to colour in this figure legend, the reader is referred to the web version of this article.)

maturation, other processes such as biological activity and diagenesis seem to have a decisive influence on the isotopic composition of S1 and S2.

In Fig. 10, isotope fractionation ($\varepsilon_{peak\text{-}genS1}$) values are compared to calculated vitrinite reflectance (Eqs. (1) and (2)) to enable an easier comparison with published data. According to Jarvie et al. (2001), the vitrinite reflectance equivalent (Vr_{eq}) can be calculated based on the T_{max} values:

$$Vr_{eq} = 0.018 \times T_{max} - 7.16 \quad (5)$$

The Vr_{eq} for all the analysed samples has a range from 0.3% Vr_{eq} to 0.9% Vr_{eq} and is therefore covers maturities from immature conditions to peak oil maturity.

The samples from the low maturity region, with no significant hydrocarbon generation, do not follow a maturity trend but are rather influenced by the original isotopic composition which is related to biological precursors and/or diagenetic processes. However, as soon as petroleum generation and expulsion become an important feature within the so-called oil window, isotope fractionation values start to exhibit a positive correlation with thermal maturity.

In the early stages of hydrocarbon generation, the isotopic values of the S1 and the T_{peak} exhibit a significant difference of up to 2.8‰ (Whitby Mudstone Fm 4). With increasing maturity, the S1 and T_{peak} isotopic values draw closer until a $\varepsilon_{peak\text{-}genS1}$ of approximately 0 (samples 8 and 9 from the Frysjaodden Fm) is

reached at Vr_{eq} value of 0.9%. This marks the point of peak oil generation.

The sample set that has been used here does not contain a complete maturity series since no samples exhibit a maturity above 1.0 Vr_{eq}. Therefore, more data are needed to support our findings. However, based on the data presented here, it is evident that even small isotopic changes within the reactive organic fraction of an OM-containing rock can be used to evaluate the maturity of the sample material and shed light on secondary processes that might have influenced the organic properties of a rock sample. Those secondary processes can be related to biological activity, either during diagenesis or biodegradation, as well as the effects of staining by oil and bitumen of sources with different origins than the sample itself.

The key advantage of this new system is the rapid isotopic measurement of thermally differentiated compound classes (free hydrocarbons and kerogen) in geological samples. This might help to generate large datasets in a shorter amount of time. The setup presented here provides a variety of analytical additions such as pyrolysis of petroleum and environmental samples. Future developments might also include measurements of $\delta^{43}S$, δD, and $\delta^{15}N$.

Measurements of isotopic differences in the oil inventory (S1) and the kerogen (S2) has strong implications for oil–source rock correlations and studies that investigate migration processes. In addition, it might be possible to evaluate the impact of drilling mud overprinting of the S1 fraction by comparing the covariance of its $\delta^{13}C$ composition with that of S2 and aliquots of drilling mud.

4. Conclusions

A new pyrolysis method has been developed which is capable of producing isotopic values for the pyrolyzable fraction of a rock sample in an online analytical system, thereby separating this fraction into S1 and S2 proportions to make the results comparable to Rock-Eval analysis. To produce a robust and reliable isotopic measurement, sulphanilamide was used as external isotopic standard. A measurement with the described system can be performed within 40–60 min and only limited sample preparation is required (removing carbonate prior to analysis). The fully automated cryogenic focusing systems makes it possible to monitor isotopic composition changes within the S2 peak. Therefore, the isotopic composition of the sample to be analysed can be monitored during the course of a fast heating experiment.

Ten samples from different locations, different depositional environments and of different maturities have been analysed with elemental analyses, Rock-Eval and the py-IRMS system. It was possible to fully characterize the reactive fraction of the OM isotopically for each sample and to monitor isotopic changes in the course of the open system pyrolysis experiment. In addition, we suggest interpretations for the isotopic fractionation curves by associating them with the respective organic matter preservation state, depositional environments and thermal maturity. We assumed that a better state of organic matter preservation is associated with an increased degree of fractionation since the original pool of ^{12}C is less affected by microbial processes during OM deposition. Sample material most likely deposited under exclusively anoxic conditions shows the most prominent isotopic fractionation of up to 3‰ between the early and the late part of the S2 signal. The results presented here and initial interpretations correspond well with previously published literature which examined the depositional environment of sample material that has been used in this study.

The isotopic signal preserved in the reactive OM fraction is affected by multiple processes such as deposition, maturity and secondary alteration. Our sample set is a first step towards a better understanding of the isotopic "bulk" characteristics of reactive OM, but does not achieve a comprehensive deconvolution of all processes and the effects involved.

Although more data are needed to fully understand the relationship between the isotopic fractionation behaviour of diverse OM fractions, we used the difference between the reactive isotopic values (S2) and the extractable fraction (S1) in order to make inferences about the thermal maturity of the different materials. We have shown that a maturity trend can be generated with these data. The difference between the S1 and S2 isotopic values draws closer until peak oil generation at approximately Vr_{eq} 0.9% is reached and where $\varepsilon_{peak\text{-}genS1}$ becomes 0. Samples that are outside of the maturity trend are likely to be immature and influenced by secondary processes such as staining or biodegradation.

The results and interpretations related to thermal maturity needs to be extended in a further study, by analysing a maturity series which covers maturities up to the late condensate and gas window. This approach might also support the development of new isotopic kinetic models for different kerogen types. The capabilities of the proposed method in oil source rock correlation tasks needs to be investigated further. In another study, we aim to compare petroleum isotopes with their corresponding source rocks at different maturity stages to predict the isotopic composition of an expelled oil with its immature source rock by employing the py-IRMS method.

Acknowledgements

The authors are grateful to the reviewers Jorge E. Spangenberg, Darren Gröcke, and Dag Arild Karlsen for providing helpful comments and suggestions making this manuscript better. The authors thank Lorenz Schwark and John Volkman for handling the manuscript. Markus Doerner thanks Equinor AS for funding his PhD project at the University of Bergen, and the possibility to perform and develop all analytical methods in the Equinor research laboratory in Sandsli, Norway. All are grateful to Equinor AS for the permission to present and publish the findings. MD thanks Marian Våge for the support with the sample preparation and Arne Hundhammer for technical support, as well as Hege Fonneland for providing access to the analytical facilities and supporting the projects.

Author's contribution

Markus Doerner conceived and designed the experimental setup. Markus Doerner performed the experiments, analysed and evaluated the data. Markus Doerner and Ulrich Berner interpreted the data. Markus Doerner, Ulrich Berner, Michael Erdmann, and Tanja Barth wrote the manuscript.

Declaration of Competing Interest

The authors declare no conflict of interest.

Appendix A. Supplementary material

Supplementary data to this article can be found online at https://doi.org/10.1016/j.orggeochem.2019.06.007.

References

Allen, P., 1975. Wealden of the Weald: a new model. Proceedings of the Geologists' Association 86 (4), 389–437.

Allen, P., 1981. Pursuit of Wealden models. Journal of the Geological Society 138, 375–405.

Andresen, B., Barth, T., Irwin, H., 1993. Yields and carbon isotopic composition of pyrolysis products from artificial maturation processes. Chemical Geology 106, 103–119.

Arneth, J.D., Matzigkeit, U., 1986. Laboratory-simulated thermal maturation of different types of sediments from the Williston Basin, North America–effects on the production rates, the isotopic and organo-geochemical composition of various pyrolysis products. Chemical Geology: Isotope Geoscience 58, 339–360.

Banerjee, A., Sinha, A.K., Jain, A.K., Thomas, N.J., Misra, K.N., Chandra, K., 1998. A mathematical representation of Rock-Eval hydrogen index vs T_{max} profiles. Organic Geochemistry 28, 43–55.

Bordenave, M.L., 1993. Applied Petroleum Geochemistry. Editions Technip, Paris.

Behar, F., Beaumont, V., Panteado, A., De, H.L.B., 2001. Rock-Eval 6 technology: performance and developments. Oil & Gas Science and Technology – Revues IFP 56, 111–134.

Berner, U., 1982. Variationen der stabilen Wasserstoff- und Kohlenstoffisotope in Erdölen. Diploma Thesis, Technical University of Clausthal-Zellerfeld, 114 pp.

Berner, U., Faber, E., Scheeder, G., Panten, D., 1995. Primary cracking of algal and land plant kerogens: kinetic models of isotope variations in methane, ethane and propane. Chemical Geology 126, 233–245.

Berner, U., Faber, E., 1996. Empirical carbon isotope/maturity relationship for gases from algal kerogens and terrigenous organic matter, based on dry, open-system pyrolysis. Organic Geochemistry 24, 947–955.

Brekke, T., Krajewski, K.P., Hubred, J.H., 2014. Organic geochemistry and petrography of thermally altered sections of the Middle Triassic Botneheia Formation on south-western Edgeøya, Svalbard. Norwegian Petroleum Directorate Bulletin 11, 111–128.

Boreham, C.J., Summons, R.E., Roksandic, Z., Dowling, L.M., Hutton, A.C., 1994. Chemical, molecular and isotopic differentiation of organic facies in the Tertiary lacustrine Duaringa oil shale deposit, Queensland, Australia. Organic Geochemistry 21, 685–712.

Carroll, A.R., Bohacs, K.M., 2001. Lake-type controls on petroleum source rock potential in nonmarine basins. American Association of Petroleum Geologists Bulletin 85, 1033–1053.

Clayton, C.J., 1991a. Effect of maturity on carbon isotope ratios of oils and condensates. Organic Geochemistry 17, 887–889.

Clayton, C.J., 1991b. Carbon isotope fractionation during natural gas generation from kerogen. Marine and Petroleum Geology 8, 232–240.

Cole, R.D., Picard, D., 1981. Sulfur-isotope variations in marginal-lacustrine rocks of the Green River Formation, Colorado and Utah. SEPM Special Publication 31, 261–275.

Cooles, G.P., Mackenzie, A.S., Quingley, T.M., 1986. Calculation of petroleum masses generated and expelled from source rocks. Organic Geochemistry 10, 235–245.

Cramer, B., Faber, E., Gerling, P., Krooss, B.M., 2001. Reaction kinetics of stable carbon isotopes in natural gas insights from dry, open system pyrolysis experiments. Energy & Fuels 15, 517–532.

Dahlgren, S., Hanesand, T., Mills, N., Patience R., Brekke, T., Sinding-Larsen, R., 1998a. Norwegian Geochemical Standard samples: Svalbard Rock-1 (NGS SR-1). Norwegian Geochemical Standards Newsletter vol. 1. Norwegian Petroleum Directorate, Stavanger, Norway.

Dahlgren, S., Hanesand, T., Mills, N., Patience R., Brekke, T., Sinding-Larsen, R., 1998b. Norwegian Geochemical Standard samples: Jet Rock-1 (NGS JR-1). Norwegian Geochemical Standards Newsletter vol. 2. Norwegian Petroleum Directorate, Stavanger, Norway.

Doerner, M., Berner, U., Erdmann M., Barth, T., 2018. Organic geochemical research analytics of the petroleum industry: enhanced data density and method flexibility using gas chromatograph multiple detector coupling. Geological Society, London, Special Publications, 484, 17 September 2018. https://doi.org/10.1144/SP484.6.

Dypvik, H., Riber, L., Burca, F., Rüther, D., Jargvoll, D., Nagy, J., Jochmann, M., 2011. The Paleocene-Eocene thermal maximum (PETM) in Svalbard – clay mineral and geochemical signals. Paleogeography, Paleoclimatology, Paleoecology 302, 156–169.

Espitalié, J., Deroo, G., Marquis, F., 1985a. La pyrolyse Rock-Eval et ses applications. Première partie. Oil & Gas Science and Technology 40, 563–579.

Espitalié, J., Deroo, G., Marquis, F., 1985b. La pyrolyse Rock-Eval et ses applications. Deuxième partie. Oil & Gas Science and Technology 40, 755–784.

Espitalié, J., Deroo, G., Marquis, F., 1986. La pyrolyse Rock-Eval et ses applications. Troisième partie. Oil & Gas Science and Technology 41, 73–89.

Espitalié, J., Laporte, J.L., Madec, M., Marquis, F., Leplat, P., Paulet, J., Boutefeu, A., 1977. Méthode rapide de caractérisation des roches mères, de leur potentiel pétrolier et de leur degré d'évolution. Oil & Gas Science and Technology 32, 23–42.

Grundvåg, S.-A., Johannessen, E.P., Helland-Hansen, W., Pling- Björklund, P., 2014. Depositional architecture and evolution of progradationally stacked lobe complexes in the Eocene Central Basin of Spitsbergen. Sedimentology 61, 535–569.

Galimov, E.M., Posyagin, V.I., Prokhorov, V.S., 1972. Experimental study of carbon isotope fractionation in the CH_4–C_2H_6–C_3H_8–C_4H_{10} system at different temperatures. Geokhimiya 8, 977–987.

Galimov, E.M., 1973. Carbon isotopes in oil and gas geology (In Russian). Moscow, Nedra, English translation, Washington, NASA TT F-682, Washington, D.C., 1975, 384 pp.

Galimov, E.M., 1975. The Biological Fractionation of Isotopes. Academic Press, Orlando, p. 261.

Galimov, E.M., 2006. Isotope organic geochemistry. Organic Geochemistry 37, 1200–1262.

Hayes, J.M., Freeman, K.H., Popp, B.N., Hoham, C.H., 1990. Compound-specific isotopic analyses: a novel tool for reconstruction of ancient biogeochemical processes. Organic Geochemistry 16, 1115–1128.

Hayes, J.M., Takigiku, R., Ocampo, R., Callot, H.J., Albrecht, P., 1987. Isotopic compositions and probable origins of organic molecules in the Eocene Messel shale. Nature 329, 48–51.

Hill, R.J., Tang, Y., Kaplan, I., 2003. Insight into oil cracking based on laboratory experiments. Organic Geochemistry 34, 1651–1672.

Howard, A.S., 1985. Lithostratigraphy of the Staithes Sandstone and Cleveland Ironstone formations (Lower Jurassic) of North-East Yorkshire. Proceedings of the Yorkshire Geological Society 45, 261–275.

Jarvie, D.M., Claxton, B.L., Henk, F., Breyer, J.T., 2001. Oil and shale gas from the Barnett Shale, Ft. Worth Basin, Texas. Abstract, American Association of Petroleum Geologists Annual Meeting Program 10, p. A100.

Jarvie, D.M., Hill, R.J., Pollastro, R.M., 2005. Assessment of the gas potential and yields from shales: the Barnett Shale model. Oklahoma Geological Survey Circular 110, 37–50.

Katz, B.J., 1983. Limitations of "Rock-Eval" pyrolysis for typing organic matter. Organic Geochemistry 4, 195–199.

Knox, R.W.O'B., 1984. Lithostratigraphy and depositional history of the late Toarcian sequence at Ravenscar, Yorkshire. Proceedings of the Yorkshire Geological Society 45, 99–108.

Komada, T., Anderson, M.R., Dorfmeier, C.L., 2008. Carbonate removal from coastal sediments for the determination of organic carbon and its isotopic signatures, $\delta^{13}C$ and $\Delta^{14}C$: comparison of fumigation and direct acidification by hydrochloric acid. Limnology and Oceanography: Methods 6, 254–262.

Lehmann, M.F., Bernasconi, S.M., Barbieri, A., McKenzie, J.A., 2002. Preservation of organic matter and alteration of its carbon and nitrogen isotope composition during simulated and in situ early sedimentary diagenesis. Geochimica et Cosmochimica Acta 66, 3573–3584.

Leventhal, J.S., 1995. Carbon-sulfur plots to show diagenetic and epigenetic sulfidation in sediments. Geochimica et Cosmochimica Acta 59, 1201–1211.

Lewan, M.D., 1983. Effects of thermal maturation on stable organic carbon isotopes as determined by hydrous pyrolysis of Woodford Shale. Geochimica et Cosmochimica 74, 1471–1749.

Lewan, M.D., 1986. Stable carbon isotopes of amorphous kerogens from Phanerozoic sedimentary rocks. Geochimica et Cosmochimica Acta 50, 1583–1591.

Li, Y., Tang, D., Fang, Y., Xu, H., Meng, Y., 2014. Distribution of stable carbon isotope in coalbed methane from the east margin of Ordos Basin. Science China Earth Sciences 57, 1741–1748.

Lorant, F., Prinzhofer, A., Behar, F., Huc, A.-Y., 1998. Carbon isotopic and molecular constrains on the formation and the expulsion of thermogenic hydrocarbon gases. Chemical Geology 147, 249–264.

Macko, S.A., Engel, M.H., Parker, P.L., 1993. Early diagenesis of organic matter in sediments. In: Engel, M.H., Macko, S.A. (Eds.), Organic Geochemistry. Springer, Boston, MA, pp. 211–224.

Matthes, G., 1968. Les couches éocènes dans la région du fosse rhénan septentrional. Mémoires de la Bureau de Recherche Géologiques et Minières 58, 327–337.

Morris, K.A., 1980. Comparison of major sequences of organic-rich mud deposition in the British Jurassic. Journal of the Geological Society 137, 157–170.

Pepper, A.S., Corvi, P.J., 1995. Simple kinetic model of petroleum formation. Part I: oil and gas generation from kerogen. Marine and Petroleum Geology 12, 291–319.

Peters, K.E., Rohrback, B.G., Kaplan, I.R., 1981. Carbon and hydrogen stable isotope variation on kerogen during laboratory-simulated thermal maturation. American Association of Petroleum Geologists Bulletin 65, 501–508.

Powell, J.H., 1984. Lithostratigraphical nomenclature of the Lias Group in the Yorkshire Basin. Proceedings of the Yorkshire Geological Society 45, 51–57.

Romero-Sarmiento, M.-F., Pillot, D., Letort, G., Lamoureux-Var, V., Beaumont, V., Huc, A.-Y., Garcia, B., 2016. New Rock-Eval method for characterization of unconventional shale resource systems. Oil and Gas Science and Technology – Revues d'IFP Energies Nouvelles 71. https://doi.org/10.2516/ogst/2015007.

Rooney, M.A., Claypool, G.E., Chung, H.M., 1995. Modelling thermogenic gas generation using carbon isotope ratios of natural gas hydrocarbons. Chemical Geology 126, 219–232.

Ruble, T.E., Philp, R.P., 1998. Stratigraphy, depositional environments and organic geochemistry of source rocks in the Green River Petroleum System, Uinta Basin, Utah. Utah Geological Association, Modern and Ancient Lake Systems: New Problems and Perspectives, pp. 289–328.

Ruble, T.E., Lewan, M.D., Philp, R.P., 2001. New insights on the Green River petroleum system in the Uinta Basin from hydrous pyrolysis experiments. American Association of Petroleum Geologists Bulletin 85, 1333–1371.

Schimmelmann, A., Mastalerz, M., Gao, L., Sauer, P.E., Topalov, K., 2009. Dike intrusions into bituminous coal, Illinois Basin: H, C, N, O isotopic responses to rapid and brief heating. Geochimica et Cosmochimica Acta 73, 6264–6281.

Schimmelmann, A., Qi, H.P., Coplen, T.B., Brand, W.A., Fong, J., Meier-Augenstein, W., Kemp, H.F., Toman, B., Ackermann, A., Assonov, S., Aerts-Bijma, A.T., Brejcha, R., Chikaraishi, Y., Darwish, T., Elsner, M., Gehre, M., Geilmann, H., Groing, M., Helie, J.F., Herrero-Martin, S., Meijer, H.A.J., Sauer, P.E., Sessions, A.L., Werner, R.A., 2016. Organic reference materials for hydrogen, carbon, and nitrogen stable isotope-ratio measurements: caffeines, *n*-alkanes, fatty acid methyl esters, glycines, L-valines, polyethylenes, and oils. Analytical Chemistry 88, 4294–4302.

Schoell, M., 1984. Recent advances in petroleum isotope geochemistry. Organic Geochemistry 6, 645–663.

Simoneit, B.R.T., Brenner, S., Peters, K.E., Kaplan, I.R., 1981. Thermal alteration of Cretaceous black shale by diabase intrusions in the Eastern Atlantic – II. Effects on bitumen and kerogen. Geochimica et Cosmochimica Acta 45, 1581–1602.

Smoot, J.P., 1983. Depositional subenvironments in an arid closed basin; the Wilkins Peak Member of the Green River Formation (Eocene), Wyoming, U.S.A. Sedimentology 30, 801–827.
Sofer, Z., 1984. Stable carbon isotope composition of crude oils: Applications to source depositional environments and petroleum alteration. American Association of Petroleum Geologists Bulletin 68, 31–49.
Somsamak, P., Richnow, H.H., Häggblom, M.M., 2006. Carbon isotope fractionation during anaerobic degradation of methyl tert-butyl ether under sulfate-reducing and methanogenic conditions. Applied and Environmental Microbiology 72, 1157–1163.
Stahl, W.J., 1978. Source rock–crude oil correlation by isotopic type-curves. Geochimica et Cosmochimica Acta 42, 1573–1577.
Stahl, W.J., Carey Jr, B.D., 1975. Source-rock identification by isotope analyses of natural gases from fields in the Val Verde and Delaware basins, west Texas. Chemical Geology 16, 257–267.
Stockar, R., Adatte, T., Baumgartner, P.O., Föllmi, K.B., 2013. Palaeoenvironmental significance of organic facies and stable isotope signatures: the Ladinian San Giorgio Dolomite and Meride Limestone of Monte San Giorgio (Switzerland, WHL UNESCO). Sedimentology 60, 239–269.
Spiker, E.C., Hatcher, P.G., 1984. Carbon isotope fractionation of sapropelic organic matter during early diagenesis. Organic Geochemistry 5, 283–290.
Surdam, R.C., Wolfbauer, C.A., 1975. Green River Formation, Wyoming: a playa-lake complex. Geological Society of America Bulletin 86, 335–345.
Tissot, B.P., Welte, D.H., 1978. Petroleum Formation and Occurrence: A New Approach to Oil and Gas Exploration. Springer.
Tocqué, E., Behar, F., Budzinski, H., Lorant, F., 2005. Carbon isotopic balance of kerogen pyrolysis effluents in a closed system. Organic Geochemistry 36, 893–905.
Waples, D.W., 1985. Geochemistry in Petroleum Exploration. Springer. 232 pages.
Whiticar, M.J., 1999. Carbon and hydrogen isotope systematics of bacterial formation and oxidation of methane. Chemical Geology 161, 291–314.
Wimbledon, W.A., Allen, P., Fleet, A.J., 1996. Penecontemporaneous oil-seep in the Wealden (early Cretaceous) at Mupe Bay, Dorset. U.K. Sedimentary Geology 102, 213–220.

Graphic design: Communication Division, UiB / Print: Skipnes Kommunikasjon AS

uib.no

ISBN: 9788230848661 (print)
9788230850329 (PDF)